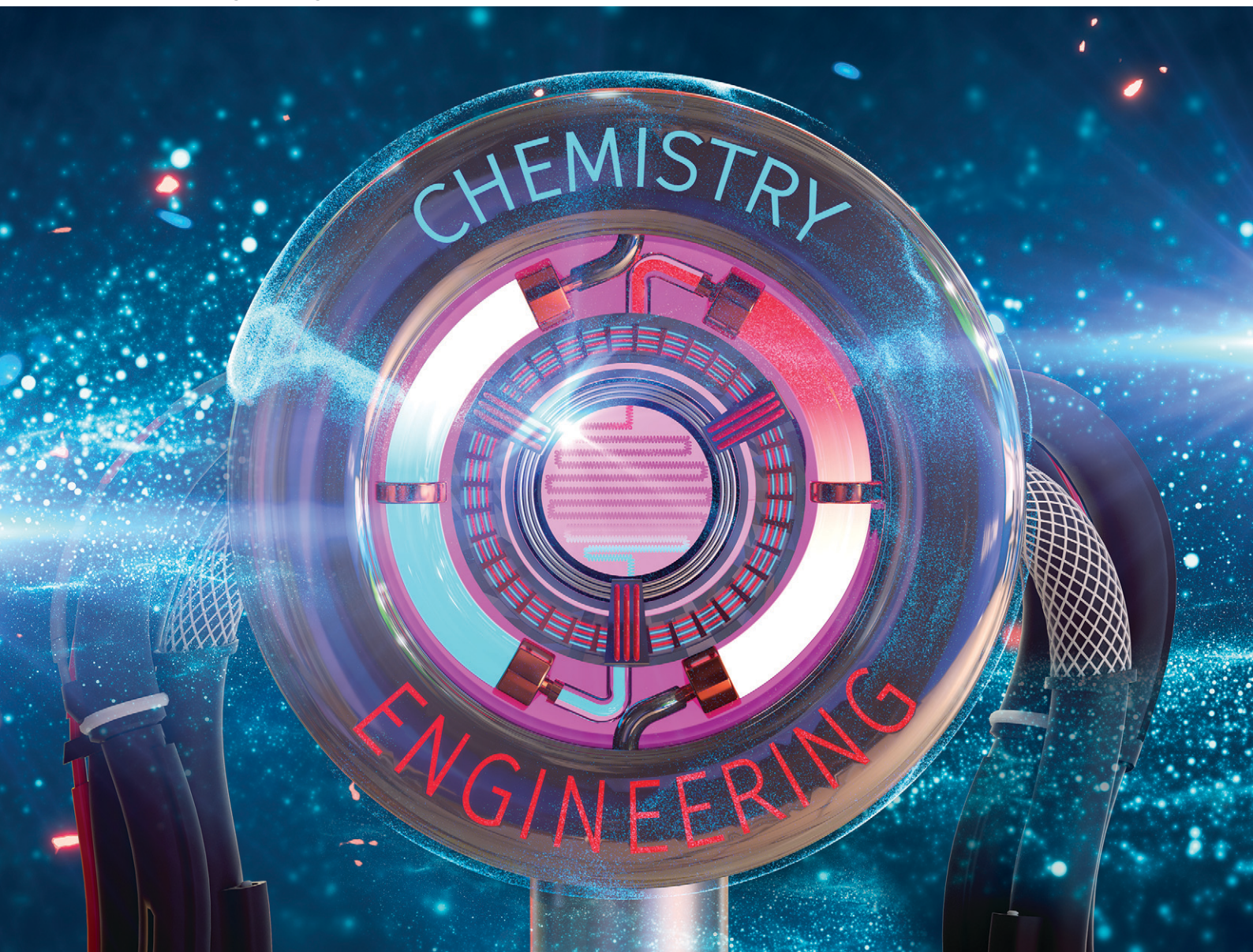


# Reaction Chemistry & Engineering

Linking fundamental chemistry and engineering to create scalable, efficient processes

[rsc.li/reaction-engineering](https://rsc.li/reaction-engineering)



ISSN 2058-9883

**REVIEW ARTICLE**

Nicole C. Neyt and Darren L. Riley  
Application of reactor engineering concepts in continuous  
flow chemistry: a review



Cite this: *React. Chem. Eng.*, 2021, 6, 1295

## Application of reactor engineering concepts in continuous flow chemistry: a review

Nicole C. Neyt  and Darren L. Riley \*

The adoption of flow technology for the manufacture of chemical entities, and in particular pharmaceuticals, has seen rapid growth over the past two decades with the technology now blurring the lines between chemistry and chemical engineering. Current indications point to a future in which flow chemistry and related technologies will be a major player in modern chemical manufacturing and the 4th industrial revolution. In this review we highlight the application of new reactor configurations and designs in the context of either bespoke or commercial flow apparatus specifically related to microwave chemistry, photochemical transformations, electrochemical promoted reactions and multi-phasic reactions. In addition, we look at how 3D printing in reactor design and computer-aided automation is growing within the field and finally describe how innovative solutions are being developed to tackle challenging down-stream processing operations.

Received 5th January 2021,  
Accepted 4th May 2021

DOI: 10.1039/d1re00004g

rsc.li/reaction-engineering

### Introduction

The past 150 years have been truly phenomenal in the field of synthetic organic chemistry. There has been unprecedented growth, affording researchers with a better understanding of the fundamentals of the discipline, the methodologies employed, and the analytical capabilities required. In addition, chemical manufacturing technologies have also grown substantially but remained largely batch-by-batch focused. These successes have not come without their consequences: environmental pollution and negative socioeconomic impacts, and at this point in time the future still holds enormous challenges for the field in terms of sustainable manufacturing, healthcare provision, lifestyle management and smarter energy solutions.<sup>1</sup>

In the past decade flow chemistry and the application of flow devices has made a fundamental impact on academic research and academic laboratories globally. It is considered a valuable alternative to traditional batch processing primarily because of its ease of use and control. Flow chemistry, microchemistry or continuous flow chemistry is the process of performing chemical reactions in a continual flowing stream.<sup>2</sup> Reactive components are pumped together at a mixing junction and flowed through a reactor (temperature controlled) to perform a specific reaction.

The vision of the FDA's pharmaceutical quality initiative for the 21st century is to create a more robust and flexible pharmaceutical sector, and the use of continuous

manufacturing is one strategy capable of meeting this vision.<sup>3</sup> As such the adoption of the technology is now supported by the Food and Drug Administration and the Green Chemistry Society, and it has been identified as one of the ten most important chemical innovations that will change the world and pave a way for a sustainable future in chemistry.<sup>4</sup>

The complementary relationship between chemistry and technology development has been highlighted by continuous flow processing over the past few years, with constant advancements in microreactor designs and architecture. This on-going growth from round bottom flasks to flow reactors has led to the integration of new concepts in mixing, dosing, heat transfer and processing in general.<sup>5</sup> In many instances, innovative bespoke engineering solutions have been developed in laboratories across the globe greatly expanding the scope of flow chemistry. In this review we have focused on the role of new reactor configurations and designs in the context of either custom-made or commercial apparatus specifically related to microwave chemistry, photochemical transformations, electrochemical promoted reactions, gas-liquid mediations, 3D printing in reactor design, computer-aided automation and down-stream processing operations. These have been the areas with the most advances in reactor designs and equipment, with the primary application range for these technologies being the synthesis of active pharmaceutical ingredients (API's). Several reviews have been written on the various topics discussed in this overview,<sup>6–13</sup> as such, we have elected to highlight key applicator concepts with a focus on recent and highly influential articles in the field.

Faculty of Natural and Agricultural Sciences, Department of Chemistry, University of Pretoria, 0002, South Africa. E-mail: darren.riley@up.ac.za



Although continuous-flow chemistry has numerous benefits, it has drawbacks and limitations as well. For example, handling of solids, precipitates and sediments can lead to the blockage of the flow system, however, in many cases these problems are mitigated through the use of solid-supported reagents, appropriate solvent choices and in certain applications through the use of larger channel sizes.

Method development can also be time consuming as a range of different reaction parameters need to be considered such as the temperature, solvent, concentration, pressure and residence time. However, once optimal conditions have been established, they can often be directly applied to similar reactions. Tailing or dispersion of reagents through the flowing solvent stream can also sometimes be a challenge when performing array type chemistry, or multi-step chemistry and finally, the relatively high cost of flow reactor platforms is still considered to be a limiting factor, particularly in academia, though in many instances the use of low-cost bespoke systems is now opening access to the field.

### 1 Microwave applications under flow conditions

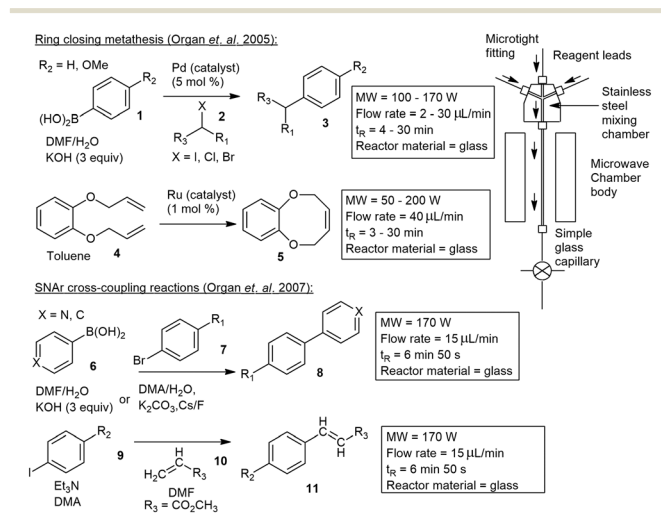
The application of microwave (MW) chemistry in flow was first realized by Strauss<sup>14,15</sup> and Chen<sup>16</sup> in the early 1990's using a quartz or Teflon based helical tube. The application of MW flow chemistry has since been widely applied to various organic reactions including nucleophilic aromatic substitutions ( $S_NAr$ ), eliminations, decarboxylations, amidations and condensation reactions. Flow technology has offered the unique ability of scaling-up procedures with microwave chemistry which had been lacking under traditional batch conditions. The major drawback associated with microwave chemistry under traditional batch conditions is the depth penetration of microwaves into the absorbing media. This is where flow microwave chemistry offers a unique advantage over batch, only a small amount of material is present at a single point in time with consistent heat transfer into the reaction media and negligible depth of penetration.<sup>6</sup> Several types of MW flow reactors are reported in literature: multimode reactors with magnetron, single mode reactors with magnetron and multi-mode reactors with a solid state oscillator. A magnetron is an electron tube designed to amplify the microwaves generated by the external magnetic field.<sup>17</sup> Most of the reported MW flow reactors have been constructed by placing a flow path within a commercially available single mode MW reactor. Several different flow paths have been reported and designed by different groups, consisting of either helical, capillary type or straight/packed tube type vessels.

Despite early uptake one could argue that MW chemistry in flow is redundant with rapid heating being achievable with suitable reactor modules. Furthermore, no new exciting evolutions have appeared in recent years with regards to the amalgamation of flow chemistry and MW heating.<sup>6</sup> That being said, we still feel that it is still pertinent to highlight a

few important concepts linked to the historical use of MW's in flow over the past ten years.

**1.1 Microwave capillary flow system.** Organ and co-workers designed a parallel capillary reactor system to demonstrate Suzuki–Miyaura and  $S_NAr$  reactions under continuous flow conditions. The microreactor was fabricated from varying sized capillary glass tubes fitted with microtight fittings onto a stainless steel (SS) mixing chamber.<sup>18</sup> Various arylboronic acids **1** were mixed together with a base in dimethylformamide (DMF) or tetrahydrofuran (THF). The mixture was pumped using a syringe pump and mixed in a stainless steel (SS) mixing chamber with the arylhalide **2** and a Pd-catalyst in DMF. A flow rate of  $15 \mu\text{L min}^{-1}$  and 170 W microwave irradiation was applied. Several substrates were investigated and the reaction products **3** were afforded in yields of 37–100% (Scheme 1). Under the same reaction conditions, they demonstrated a ring closing metathesis with the transformation of **4** to **5** in 35% conversion. In a separate paper the same group extended the scope of Suzuki–Miyaura couplings and demonstrated Heck reactions.<sup>19</sup> In this instance the capillaries were coated with a Pd-catalyst. An aryl boronic acid moiety **6** and an aryl halide **7** were passed through the capillaries, in the presence of a suitable base and DMF or dimethylacetamide (DMA) to form the cross coupled products **8**. The Heck coupling was demonstrated when aryl iodides **9** and acrolein derivatives **10** were passed through the capillary reactor to form the coupled Heck products **11** in yields ranging from 59–97% (Scheme 1).

Similar capillary-based microwave flow reactors have been reported.<sup>18–22</sup> A capillary based microreactor was used in the oxidation of benzyl alcohol to benzaldehyde and reported by Varma and co-workers. They made use of a narrow microchannel device consisting of two main parts: an aluminium section and a polytetrafluoroethylene (PTFE) section. The reactor design allowed reactions to be carried out under isothermal conditions while being exposed to MW



**Scheme 1** Microwave-assisted continuous-flow organic synthesis (MACOS) utilizing a glass capillary reactor with Pd and/or Ru catalysts.

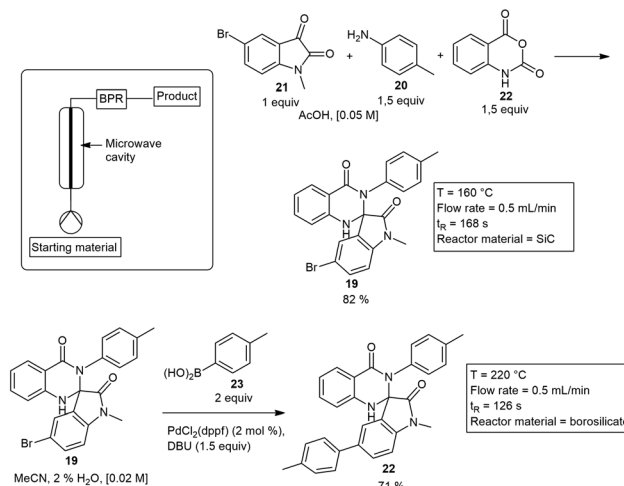


irradiation. A flow rate of 4 mL min<sup>-1</sup> equating to 75 second residence time, produced 96% conversion to benzaldehyde.<sup>23</sup>

**1.2 Channel and packed bed microwave reactors.** The application of tubular or packed bed reaction vessels have become increasingly popular due to the specific advantages offered, allowing for prolonged residence times, uniform heating and the potential for scale up of reactions.

*Straight tube inserts.* Wood and co-workers developed a simple means of performing microwave assisted continuous flow organic synthesis (MACOS) under flow conditions. They used a Pyrex tube with two drilled frits and a custom metal head fitted with a standard inlet tube and outlet fitting. The tube was filled with sand as a dispersive agent but could also be replaced with a catalyst of choice. With this they investigated the hydrolysis of chloromethylthiazole **12** to give alcohol **13** and the Fischer indole synthesis of **14** from hydrazine **15** and cyclohexanone **16** in glacial acetic acid. Efficient conversions were achieved at 150 °C, processing 1 g in 15–30 min, with products **13** and **14** afforded in 85% and 91% yield respectively (Scheme 2). Finally, they investigated a Bohlmann–Rahtz synthesis of **17** from **18** which was achieved in a 98% yield.<sup>24</sup>

A silicon carbide (SiC) tubular reactor as well as a borosilicate glass reactor has been developed by WaveCraft AB Ltd. These reactors formed part of their ArrheniusOne system which was used by Larhed and co-workers to synthesize spiro-oxindole dihydroquinazolinones known as insulin regulated aminopeptidase (IRAP) inhibitors.<sup>25</sup> The route involved a MW flow synthesis to build a library of spiro-cyclic compounds **19**, from a three component reaction involving **20**, **21** and **22**. These spiro-cycles were synthesized in yields varying from 40–87% yield. This was followed by a Suzuki–Miyaura cross coupling reaction with phenylboronic acid **23** to form the potential IRAP inhibitor **22**, the product was formed in 71% yield with Pd-catalyst (Scheme 3). Further publications also demonstrated a range of Suzuki–Miyaura couplings in excellent yields with the same SiC MW flow vessel.<sup>26</sup> A similar quartz tubular reactor was designed by Suzuki and co-workers demonstrating rapid heating of solvents at pressures up to 10 MPa. Polar solvents such as

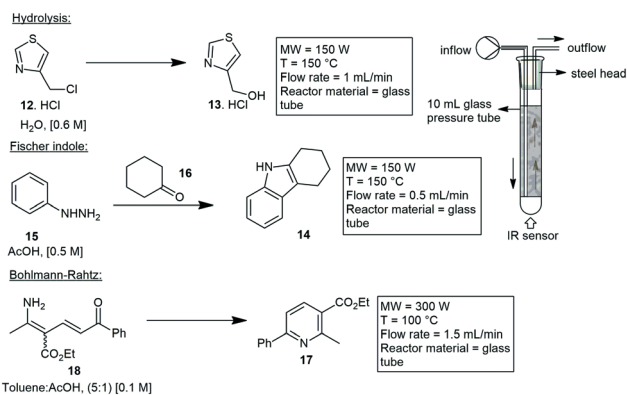


**Scheme 3** Microwave heated flow synthesis of spiro-oxindole dihydroquinazolinone based IRAP inhibitors utilizing a borosilicate and SiC MW vessel.

water, ethylene glycol and ethanol were heated instantaneously to temperatures above their boiling points by applying pressure. They also demonstrated the rapid synthesis of Cu-nanoparticles by elevating the reaction temperature of ethylene glycol.<sup>27</sup>

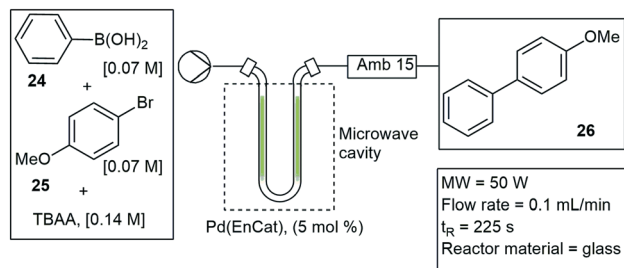
Koloini and co-workers were one of the first groups to perform MW reactions under flow conditions. In 1999 they designed a fixed bed MW reactor packed with a solid supported ion resin to catalyse esterification reactions. They used a conventional microwave unit from Osaka, Japan called the Panasonic NE-1780. The temperature of the outlet was measured with a Ni–Cr thermocouple. The esterification of benzoic acid was performed by passing the reaction mixture through an ion exchange resin in the presence of excess ethanol to form ethyl benzoate. The optimized flow reaction conditions were: 140 °C and 7 atm. Reaction times were significantly decreased, which typically occurred over several days at 80 °C under conventional methods.<sup>28</sup> Similarly Sajiki and co-workers demonstrated Mizoroki–Heck reactions with an immobilized Pd-catalyst supported on an anion exchange resin (DIAION WA30). The reaction was conducted in a straight tube reactor, designed by SAIDA FDS Inc. The supported catalyst was housed in this cartridge and exposed to MW irradiation.<sup>29</sup> Various iodoarenes were converted to their equivalent cinnamates in excellent yields, while the cartridge could be reused for at least 5 runs without exchange.<sup>30</sup>

*U-tube reactor insert.* Tranmer and co-workers developed a method to perform Suzuki–Miyaura couplings under MW irradiation. The method involved the use of a U-tube reactor constructed out of glass and packed with an encapsulated Pd-catalyst (Pd-EnCat). The optimized reaction conditions for the Suzuki–Miyaura couplings were set at: 5 mol% Pd-EnCat, 3 equivalents of potassium carbonate and a solvent mixture of toluene, water and ethanol (4:2:1) at elevated temperatures of 120 °C. They studied the simple reaction between



**Scheme 2** Hydrolysis and Fischer indole transformations using microwave assisted continuous flow chemistry.



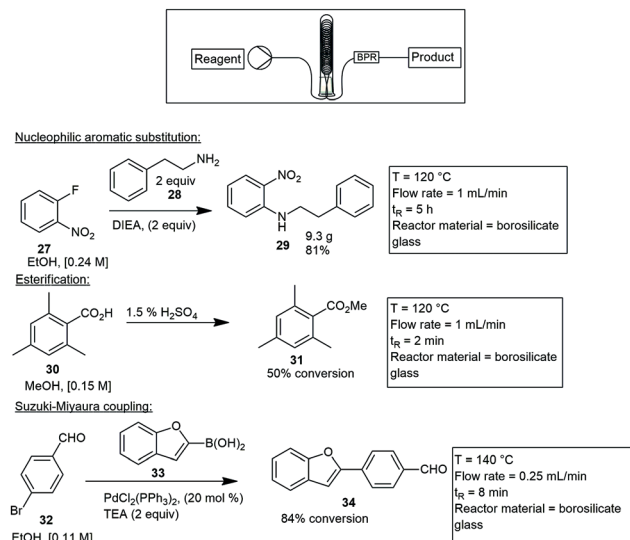


**Scheme 4** U-tube microwave insert for the application of Suzuki-Miyaura couplings under continuous flow conditions.

phenylboronic acid **24** and bromoanisole **25** and achieved 98% conversion to **26**. The reaction time was reduced from 8 h under standard batch conditions to 10 min in flow (Scheme 4).<sup>31</sup> A commercial microwave heating system, EMRYS Synthesizer Tm., was used and the U-tube glass applicator was inserted inside the MW cavity. A similar design was shown by Fletcher and co-workers in 2004, with a U-tube glass capillary and a solid supported Pd-catalyst. The catalyst was embedded inside the U-tube glass applicator and lowered inside the MW cavity. Suzuki-Miyaura couplings were performed under several reaction conditions. Optimized conditions were determined as 90 W, 80 °C MW heating, a Pd/Al<sub>2</sub>O<sub>3</sub> catalyst and potassium carbonate as base, with a 99% conversion to the coupled products.<sup>32,33</sup>

**Coiled or helical inserts.** Coiled or channel-based reactors have also frequently been used. They allow for longer residence times and faster flow rates. Reactor walls are usually coated or simply packed with a catalyst. A microwave assisted Cu-catalyzed Ullmann ether synthesis was developed by Schouten and co-workers in 2012, using a coiled type glass reactor.<sup>34</sup> The reactor walls were coated with a Cu/ZnO catalyst or alternatively, packed with a Cu/TiO<sub>2</sub> catalyst. The reaction between phenol and 4-chloropyridine was studied. Productivities of the reaction were recorded after 6 h at 28.3 and 55.1 kg h<sup>-1</sup> for the Cu/ZnO and Cu/TiO<sub>2</sub> respectively. Roth and co-workers followed suit and built a similar coiled glass insert. The reactor consisted of 22, 3 mm internal diameter (ID) borosilicate glass coils encased in a 100 mm × 10 mm protective borosilicate glass sheath, with a total reaction volume of 4 mL. A series of representative reactions were investigated which included a nucleophilic aromatic substitution combining 2-fluoronitrobenzene **27** with 2-phenylethanamine **28** to form **29**. An esterification reaction of arylbenzoic acid **30** in methanol (MeOH) to form **31** with a 50% conversion and finally, a Suzuki-Miyaura coupling where 4-bromobenzaldehyde **32** and boric acid **33** were coupled to form **34** with a conversion of 84%. In all cases product yields were greater or equivalent to those produced under conventional heating methods, with the ability to directly scale these reactions (Scheme 5).<sup>35</sup>

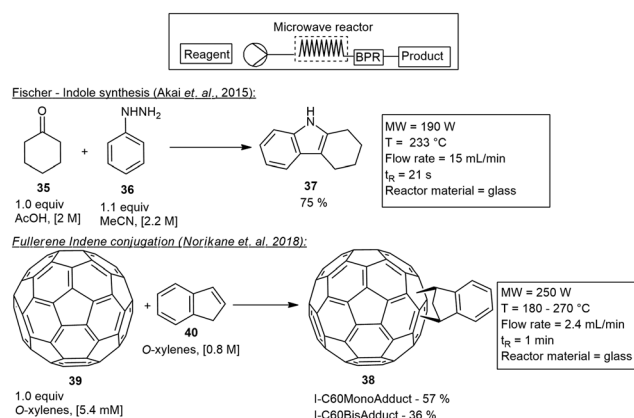
In 2015 Akai and co-workers developed a microwave reactor insert that was suitably applied to a wide variety of reactions. This applicator consisted of a wide long helical glass tube with a 3.6 mm ID and an internal volume of 5.5–6



**Scheme 5** A practical continuous flow microwave cell for nucleophilic substitutions, esterifications and Suzuki-Miyaura couplings.

mL. The glass tube was covered with PTFE tubular film for safety and insulation. To validate the function of the MW insert they studied both a Fischer indole reaction and a Diels-Alder reaction. The Fischer indole synthesis involved cyclohexanone **35** and phenylhydrazine **36** treated under MW irradiation to form carbazole **37** on a 100 g scale in 75% yield, with a residence time of 24 s.<sup>36</sup>

The microwave applicator has since been commercialised by SAIDA FDS Inc., and several reactions including ammonium salt-accelerated hydrazinolysis of unactivated amides,<sup>37</sup> Fischer esterification,<sup>36</sup> alcohol acetylation reactions,<sup>38</sup> Suzuki-Miyaura couplings, dehydrogenative aromatizations,<sup>30</sup> Wolff-Staudinger cascade reaction,<sup>39</sup> Williamson esterification,<sup>40</sup> C-alkylations of *N*-alkylamides<sup>41</sup> and a Johnson-Claisen rearrangement<sup>42</sup> have all been tested and demonstrated utilizing this insert. One of the more notable reactions performed was the scalable and selective



**Scheme 6** Various reactions demonstrated under continuous microwave conditions utilizing the SAIDA FDS Inc. insert.



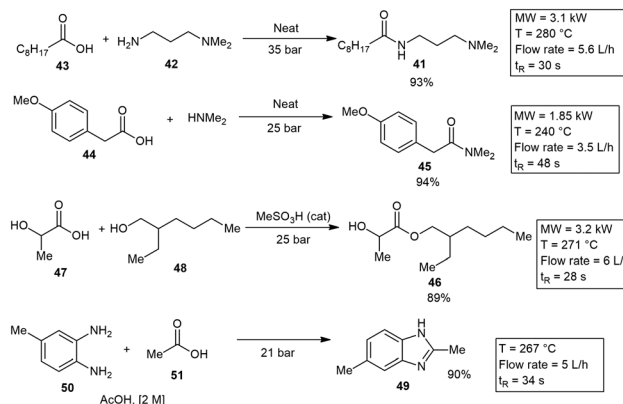
synthesis of C<sub>60</sub>/indene monoadducts **38** from the C<sub>60</sub> fullerene **39** and indene **40**.<sup>43</sup> The 5.2 mL helical reactor tube was used at a temperature of 180–270 °C, to form the indene C-60 monoadduct and bisadduct **38** in 1.1 g h<sup>-1</sup> and 0.5 g h<sup>-1</sup> respectively (Scheme 6).

**1.3 Commercial flow microwave reactors.** Several commercial flow microwave reactors have been developed, the Milestone FLOWSYNTH reactor can operate under pressures of 30 bar, temperatures of up to 230 °C with a power output of 1600 W. It consists of a 200 mL PTFE tubed coil reactor, placed inside a microwave cavity. In 2010 Moseley and co-workers<sup>44</sup> demonstrated six different reactions on industrial scale using this reactor namely: *ortho*-Claisen rearrangements, naphthofuran formations, Heck reactions, alkylation reactions and nucleophilic aromatic substitutions all of which were performed with production rates of 1–6 L h<sup>-1</sup> (0.5–3 mol h<sup>-1</sup>). A similar paper published by Moseley and Woodman demonstrated six different reactions under microwave flow conditions using the CEM Voyager SF microwave flow reactor, which operates in a stop start fashion and is considered a hybrid flow-batch microwave reactor, with reactions occurring in series unlike some microwave reactors where reactions occur in parallel.<sup>45,46</sup> The article highlighted the benefits of the CEM Voyager reactor demonstrating *ortho*-Claisen rearrangements and benzofuran formations, a Heck reaction, a hydrolysis reaction of *S*-thiocarbamates and an alkylation reaction, all on a pilot plant scale. Daily throughputs of between 50–250 g were reported with productivities ranging between 0.5–1.5 kg per day. A similar pilot plant MW reactor was designed and built by MLS GmbH & Co. KG named the ETHOS PILOT 4000, the reactor was built to operate at pressures of 60 bar, temperatures of 240 °C and flow rates of 0.2–20 L h<sup>-1</sup>. The esterification of linalool was performed on a 25 kg scale with a 2.2 L h<sup>-1</sup> flow rate.

Morschhäuser and co-workers reported on another industrial scale MW reactor demonstrating several organic reactions on large scale.<sup>47</sup> The industrial reactor was designed to operate at temperature of 310 °C and pressures of 60 bar. It was constructed from a chemically resistant, transparent, and cylindrical material made of  $\gamma$ -Al<sub>2</sub>O<sub>3</sub>. The MW reactor operated at 0.6–6 kW and demonstrated a 3.5–6 L h<sup>-1</sup> throughput. The first reaction investigated was a simple amide coupling to form **41** from a readily available amine substrate **42** and carboxylic acid derivative **43**. The amide **41** was produced in a yield of 93%. Another reaction involved the transformation of carboxylic acid **44** to amide **45** in the presence of dimethylamine. They also demonstrated the formation of a Fischer ester **46** with 2-hydroxypropanoic acid **47** and 2,2-ethyl hexanol **48** in 89% yield. Finally, the formation of imidazole **49** was achieved in 90% yield with aniline **50** and carboxylic acid **51** as substrates (Scheme 7).<sup>47</sup>

## 2 Flow photochemistry applications

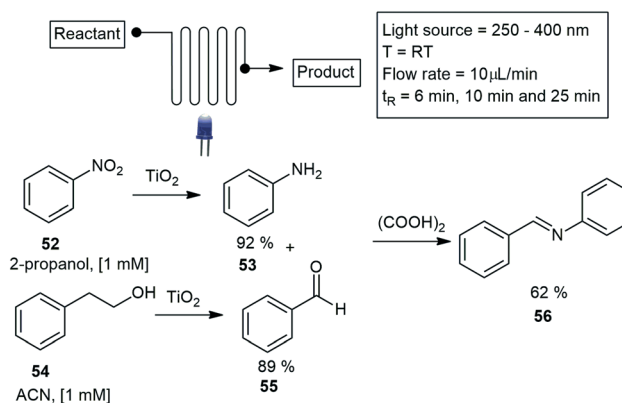
The use of light in chemical reactions has been dated back to the 18th century, but as with MW reaction, limitations



Scheme 7 Microwave assisted continuous flow on industrial scale.

associated with depth of penetration of, in this case photons into reaction media held back the widespread adoption of the technique. Recently applications of light harvesting in continual flowing streams has sparked a renaissance in the photochemistry community, with significant interest being poured into the field with the focus on the design and application of light in flow chemistry. The efforts in this field have further stimulated the development of both novel photocatalysts and photon transport improvements.<sup>48</sup>

**2.1 Microchip photo reactors.** Katayama and co-workers custom built a glass microchip reactor through a milling process. The microchip channel width was reported as 2 mm and the length 250 mm, corresponding to a reactor volume of 250  $\mu$ L. The reduction of nitrobenzene **52** to aniline **53** as well as the oxidation of benzyl alcohol **54** to benzaldehyde **55** was investigated by UV light irradiation, in a TiO<sub>2</sub> coated microchannel reactor. Furthermore, the imine **56** was produced in 62% yield by combining **53** and **55** in a continuous stream and irradiating the reaction mixture with UV light (Scheme 8).<sup>49</sup> Qin and co-workers have used a similar approach to construct a TiO<sub>2</sub> microfluidic reactor for photocatalysis and demonstrated several photocatalytic reactions.<sup>50</sup>



Scheme 8 The oxidation and reduction reactions with a milled glass microchip reactor.



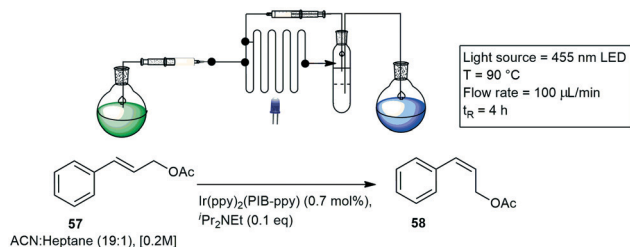
Similarly, Reiser and co-workers developed a novel photocatalytic method for the *E/Z* isomerisation of cinnamyl acetate **57** and translated this to a custom single layer continuous flow setup. The reaction involved the use of an Asia dual pump and custom glass microchip reactor irradiated with blue light emitting diode (LED) light. A novel polyisobutylene tagged iridium catalyst was also synthesized, the catalyst was recycled in a continuous fashion. The photocatalytic isomerisation of cinnamyl acetate **57** to (*Z*)-3-phenylallyl acetate **58**, was investigated, with a *Z/E* ratio of 82 : 18 achieved in 4 h (Scheme 9).<sup>51</sup>

The multigram production of hypericin was carried out using an inexpensive Pyrex® based microchip photoreactor. The photoreactor unit consisted of four or more modules connected in series. This allowed for the quantitative photocyclization of protohypericin **59** to hypericin **60**. The reactor was designed to allow variable light sources to be tested, however they found full conversion to hypericin **60** with red LED's in only 79 min (Scheme 10). Several microchip based photoreactors have been fabricated with similar materials and dimensions.<sup>52</sup>

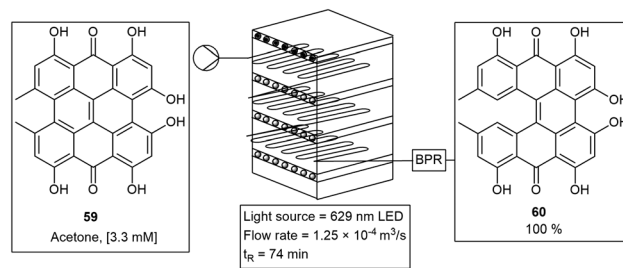
## 2.2 Microchannel or capillary type flow photoreactors

**Coiled channel reactors.** Coiled type photoreactors are the most common and accessible photoreactor systems for flow photochemistry applications. Several diverse coiled reactors have been reported in the last decade. Photocatalysis reactions in flow have been gaining interest with most being catalysed by LED's. Seeberger and Bou-Hamdan published a visible light mediated flow paper using a Ru(bpy)<sub>3</sub><sup>2+</sup> complex as a catalyst. The reactions performed with 10 to 15-fold improvement over the conventional batch method. The reactions tested included the reduction of an aromatic azide **61** to the corresponding amine **62**, the dehalogenation of  $\alpha$ -chlorophenyl acetate **63** to **64**, the opening of chalcone- $\alpha$ ,  $\beta$ -epoxide **65** to **66** and the bromination of alcohols **67** to the corresponding brominated products **68**. All reduction reactions were completed using two 17 W white LED lights, with PTFE tubing wrapped around two vertical metal rods immersed between the two LED lights. Reactions tested were performed in DMF and proceeded with 100% conversions with residence times under  $\leq 30$  min (Scheme 11).<sup>53</sup>

Another coil reactor was designed by Telmesani and co-workers in an effort to produce cyclobutanes from the dimerization of various cinnamic acids. The cone shaped

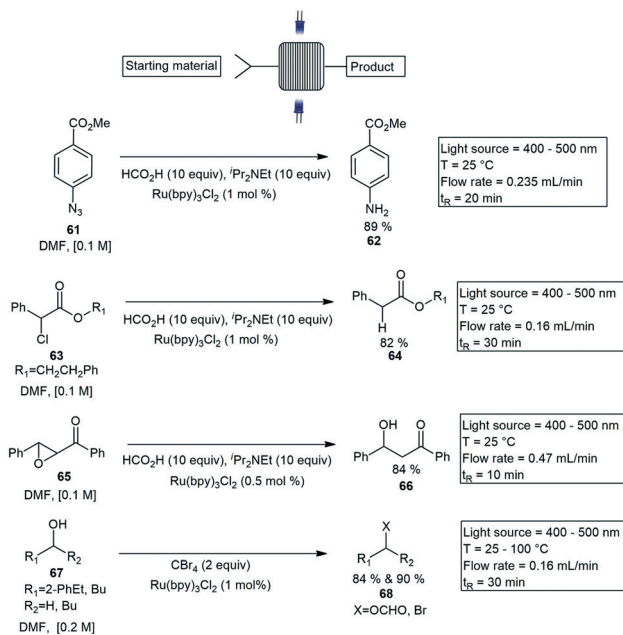


**Scheme 9** The isomerisation reaction of cinnamyl acetate under photocatalytic conditions with a glass microchip reactor irradiated with blue LED's.



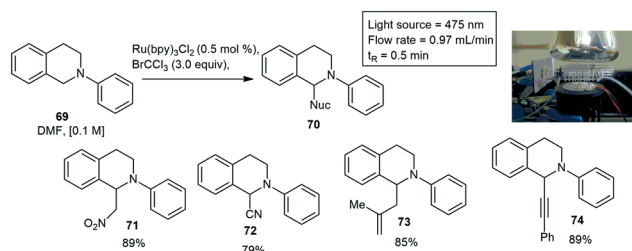
**Scheme 10** Synthesis of hypericin on multigram scale using a multimode photoreactor.

photo reactor consisted of fluorinated ethylene propylene (FEP) tubing wrapped around the photoreactor in small grooves that promote heat transfer. The temperature of the reactor was controlled by a circulating chiller. Moderate yields between 19–69% were reported with a residence time of 8 h.<sup>54</sup> The oxidative generation of iminium ions **69** from *N*-tetrahydroisoquinolines **70** using BrCCl<sub>3</sub> as terminal oxidant and Ru(bpy)<sub>3</sub><sup>2+</sup> as catalyst has also been reported. The photoreactor design included polyfluoro alkoxy (PFA) tubing wrapped in a figure eight around two glass test tubes with seven blue LED's emitting irradiation on either side. Complete conversion to the desired iminium ion was achieved in less 0.5 min residence time. The iminium ion was trapped and processed with a nucleophile such as nitromethane. Various nucleophiles were used which produced **71–74** in yields ranging between 79–89% (Scheme 12).<sup>55</sup> Huvaere and co-workers designed a similar photoreactor, consisting of FEP tubing, of 2.5 mL or 6.0 mL, a 0.8 mm ID, and a 1.6 mm outer diameter (OD) wrapped on a metal frame (8 × 10 cm). A 20 watt LED lamp or a 50 watt



**Scheme 11** Custom built microchannel reactor for photocatalytic reactions.



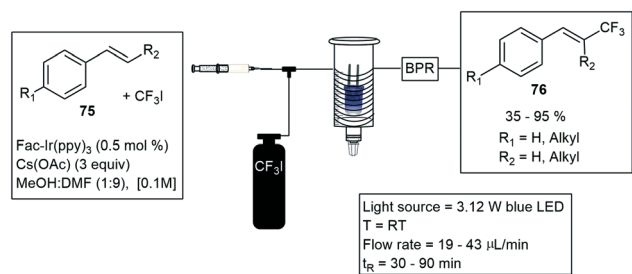


**Scheme 12** The formation of an iminium ion trapped with various nucleophiles using a custom built photoreactor under flow conditions. Photograph reproduced with permission.<sup>55</sup>

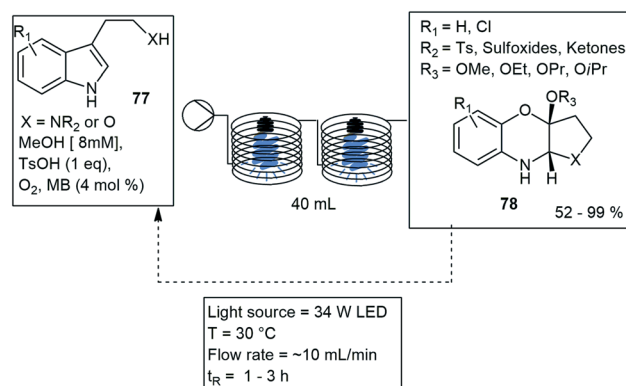
LED lamp was positioned at a distance of 0.5 cm from the photoreactor and used for the irradiation of the reaction mixtures.<sup>56</sup>

Wriedt and co-workers recently published their work on the experimental determination of photo fluxes in a multilayer channel reactor.<sup>57</sup> They studied the benefit of adding more layers to the photoreactor using actinometry and the decomposition of  $[\text{Fe}(\text{C}_2\text{O}_4)_3]^{3-}$ , carbon dioxide and oxalate. They showed that on average the ratio between the absorbed and available photons in the inner layer was 11%, for the middle layer 3% and 1% for the outer layer. More research has been focused into multilayer capillary photoreactors especially by Elliott and co-workers and Rehm and co-workers, who have already made a significant contribution in the field.<sup>58–60</sup>

Noel and co-workers constructed a simple photochemical microreactor for gas–liquid photoredox catalysis using visible light. The microreactor was constructed with high-purity PFA capillary tubing having a 0.75 mm ID and 1/16 inch OD and a total volume of 1.1 mL volume, the tubing was coiled around a disposable plastic syringe coated with refractive aluminium tape. An array of LED's was wrapped around the reactor, and the whole assembly was fixed in a larger diameter disposable plastic syringe. They reported the formation of trifluoromethylated heterocycles and thiols.<sup>61</sup> Furthermore, trifluoromethylation and hydrotrifluoromethylation protocols were described a year later, for various vinylarene substrates **75**. The method involves the use of  $\text{Fac-Ir}(\text{ppy})_3$ , visible light and inexpensive  $\text{CF}_3\text{I}$  to produce the trifluoromethylated styrenes **76** (Scheme 13). The use of continuous-flow photochemical



**Scheme 13** Trifluoromethylations under visible light conditions using a simple syringe to promote a coiled reactor under flow conditions.

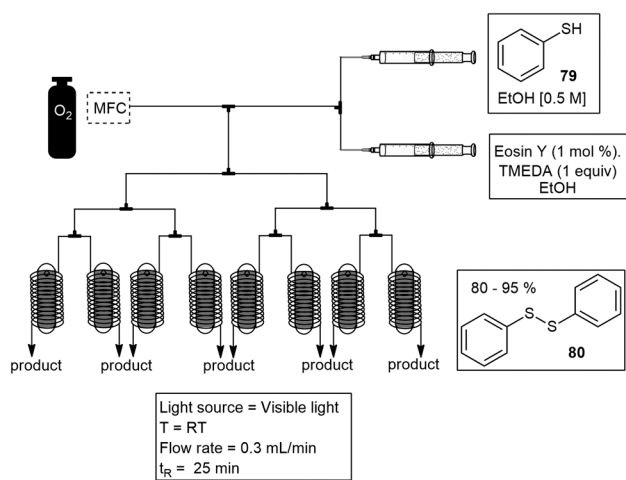


**Scheme 14** The one pot synthesis of tricyclo-1,4-benzoxazines under flow conditions using two photo reaction towers connected in series.

reaction conditions allowed for reduced residence times and increased reaction selectivity.<sup>62</sup>

A one-pot synthesis of tricyclo-1,4-benzoxazines **78** has been developed *via* metal free intramolecular cyclization of indole derivatives **77**. The reaction utilized visible light photoredox catalysis under flow conditions. Two 20 mL “reaction towers” were connected in series, each contained an LED corn light bulb (34 W) in the centre of the tower, tubing was wrapped around these for optimal light penetration (Scheme 14). The reaction occurred with the use of methylene blue (MB) in 4 mol%, toluene sulfonic acid and oxygen. The reaction proceeded quantitatively in 24 h under batch conditions and 3 h under recycling flow conditions. Various substrates were synthesized and produced in nearly quantitatively yield.<sup>63</sup>

Su and co-workers have conveniently developed a numbering up strategy for the convenient scale up of photochemical reactions. The 8 capillary system was designed to allow gas–liquid photoreactions to occur in parallel. The aerobic oxidation of thiols **79** to disulfides **80**, was used as a model reaction. The yield obtained for the



**Scheme 15** Numbering-up strategy for large scale flow photochemical synthesis.



numbering up strategy was comparable to the yield obtained in a single device (Scheme 15).<sup>64</sup>

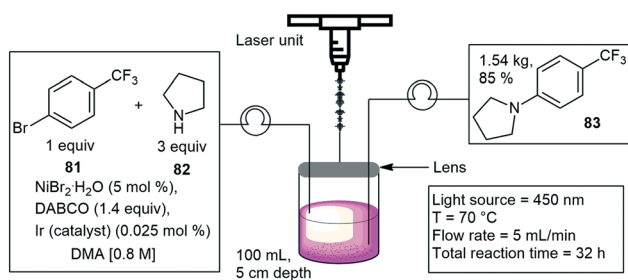
Recently Smith and co-workers synthesized a library of benzo-[1,3]oxazepines by combining the CH-activation and functionalization with photochemical heterocyclic metamorphosis. The *N*-oxide substrate was dissolved in toluene and passed through a 10 mL PFA coil, wrapped around a 25 W Exo Terra UVB200 lamp. A 100% conversion to the product was realized in only 6 min, and the product was isolated in near quantitative yield. Ten substrates were investigated with varying aromatic groups and yields between 75 and 99% were obtained within a 10 min residence time.<sup>65</sup>

**Quartz microchannel reactor.** Shen and co-workers developed a unique flow photoreactor employing quartz tubing and an aluminium mirror to perform photo-induced electron transfer deoxygenation reactions specifically to produce 2'-deoxy and 2,3'-deoxynucleosides. They showed significant improvement in the efficiency and selectivity of the reaction. Customised quartz coils and a 450 W medium pressure Hg lamp, was used to produce various nucleosides in yields ranging from 62–85%, with residence times that varied from 5–20 min.<sup>66</sup>

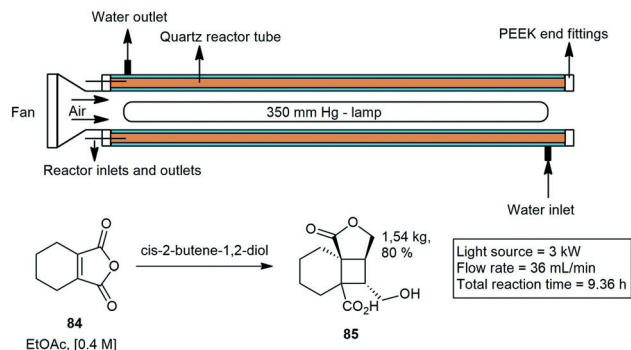
**Straight tube reactors.** A similar quartz photoreactor was designed by Kim and co-workers. Ten HPFA capillaries were filled with an immobilized eosin catalyst and housed inside the quartz jacket. These capillaries were irradiated by surrounding green LED's wrapped around them. A library of indazole based products were produced by passing a mixture of 2*H*-indazole and a tetrafluoroborate salt through the capillary photoreactor at a flow rate 2 mL min<sup>-1</sup> (0.63 min).<sup>67</sup>

Harper and co-workers have designed a photochemical reactor with the use of a laser system to promote organic reactions with more selectivity and reactivity. The reactor was fitted with a laser beam focused onto a continuous stirred tank reactor. The reactor operates in a semi-batch fashion, whereby materials are continuously fed into a stirred tank and removed as the reaction progresses. They investigated a C(sp<sup>2</sup>)-N(sp<sup>3</sup>) cross coupling reaction between 1-bromo-4-(trifluoromethyl)benzene **81** and pyrrolidine **82** to form **83** (Scheme 16).<sup>68</sup>

Elliott and co-workers developed a tubular photo reactor to perform reactions on kilogram scale. They demonstrated several organic reactions. The 120 mL reactor consisted of a



**Scheme 16** Laser mediated cross coupling reaction inside a tube reactor.

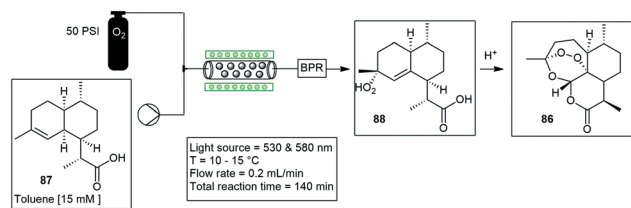


**Scheme 17** Cyclization reactions demonstrated in a straight tube quartz photo reactor.

succession of quartz tubes connected in series and arranged axially around a variable power mercury lamp. They showed that 3,4,5,6-tetrahydrophthalic anhydride (THPA) **84** and *cis*-2-butene-1,4-diol can undergo an efficient [2 + 2] cycloaddition–lactonisation sequence to afford tricyclic lactone **85** upon direct UV irradiation with a staggering production of 4 kg in 24 h. They further demonstrated similar a cyclization with productions of kilograms per day (Scheme 17).<sup>58</sup>

**2.3 Packed bed reactors.** continuous flow photoiodation method has been developed by Kong and co-workers making use of a unique packed bed reactor with immobilized rose bengal. Their photoreactor allows for the direct processing of the material without the need for further purification. Rose bengal was immobilized in a column reactor. Oxygen was fed into the system at a flow rate of 5 mL min<sup>-1</sup> and the substrate at a flow rate of 0.1 mL min<sup>-1</sup>. They demonstrated a wide scope of singlet oxygen cycloadditions and heteroatom oxidations with yields ranging from 75–98%. Furthermore, they applied their method as a strategic element in the synthesis of the high-volume antimalarial artemisinin **86** from dihydroartemisinic acid **87** and **88** (Scheme 18).<sup>69</sup> A similar photoinduced packed bed system was introduced by Tobin and co-workers, they synthesized a novel benzothiadazole (BTZ) polymer for oxidative organic transformations.<sup>70</sup>

**2.4 Unconventional reactor designs.** Noel and co-workers have made use of solar energy to perform chemical reactions, in their pioneering work they developed luminescent solar concentrator photomicroreactors (LSC-PMs). In 2016 they published a paper entitled a leaf inspired photomicroreactor, the photoreactor was built with fluorescent dye-doped



**Scheme 18** Cyclisation reactions demonstrated in a straight tube quartz photo reactor.



polydimethylsiloxane (PDMS), which harvests the sunlight, focusses the energy, and transports it to the microchannels wherein the reagents are converted. Scalability was demonstrated by means of a numbering-up strategy. They demonstrated the oxygen-mediated cycloaddition of 9,10-diphenylanthracene using MB as the photocatalyst and acetonitrile as the solvent at room temperature.<sup>71</sup> In 2019 they improved the chemical stability and manufacturing, and demonstrated the device on several reactions including the hydroxylation of phenylboronic acid to phenol, the oxidation of (L)methionine, the oxidation of benzylamine,  $\alpha$ -terpinene oxidation and morpholine arylation (Fig. 1).<sup>72</sup>

Clark and co-workers designed a photoreactor that generates a thin film upon rotation for efficient irradiation. The photoreactor comprises of a rotary evaporator with banks of LED lights mounted above the surface of the rotating evaporation flask. They demonstrated three different photooxidation reactions, and investigated several parameters which included the flask size, volume, rotation speed, and light intensity. The first reaction investigated was a photodesymmetrization of benzene-1,4-diboronic acid **89** to the mono and dihydroxylated products **90** and **91**. A 10 min residence time gave nearly quantitative conversion of the starting material **89**. The second reaction investigated was the photooxidation of  $\alpha$ -terpinene **92** to form ascaridole **93** with the highest yielding and fastest time of 87% yield in 60 seconds. The final reaction investigated was the photooxidation of citronellol **94** to form hydroperoxides which is further reduced to form the corresponding diols followed by the dehydrative cyclisation to yield rose oxide **95**. The reaction proceeded to 99% conversion in 420 seconds (Scheme 19).<sup>73</sup>

Ioannou and co-workers made use of a modified continuous flow reactor for biphasic photooxygenation reactions. The reaction solution was nebulized, using either oxygen or air, and the resulting aerosol is irradiated by an LED jacket that surrounds a Pyrex reaction chamber. They showed the formation of complex functionalised  $\gamma$ -lactams in a 4-step synthesis, with the first step involving the photocatalysis reaction, in 49–66% yield from simple furans.

Continuous photo-oxidation reactions have further been reported in vortex reactor systems. The vortex reactor makes use of a rapidly rotating cylinder to generate Taylor vortices

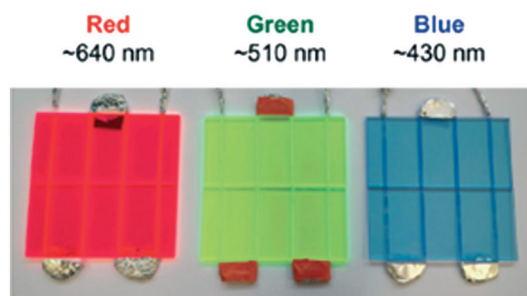
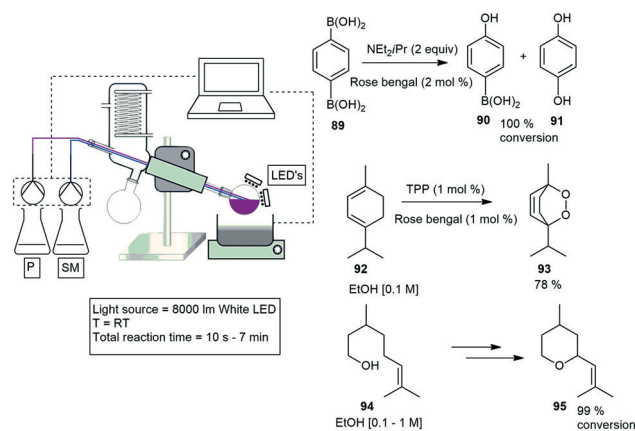


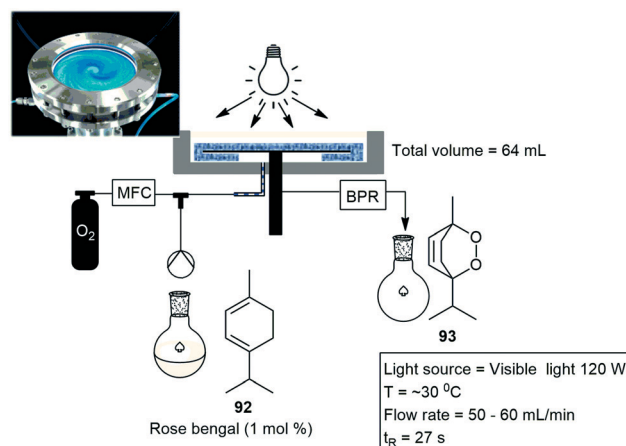
Fig. 1 Luminescent solar concentrator photomicroreactors by Noel and co-workers. Photograph reproduced with permission.<sup>72</sup>



Scheme 19 Photo oxidation reactions using a common rotary evaporator.

for continuous thermal and photochemical reactions. The vortex reactor has been applied to several organic photochemical reactions including the oxidation of  $\alpha$ -terpinene **92** to ascaridole **93** in 91%, furfuryl alcohol to furfuraldehyde in 73% as well as the photodeborylation of phenylboronic acid to phenol in 94% yield. The rotation speed was key to the reaction efficiency, demonstrating the highest efficiency at 4000 rpm, allowing for optimal absorption of air. The reactor was further applied to the oxidation of artemisinin in quantitative conversion and a yield of 50%.<sup>74</sup>

Another unconventional photoreactor named the photo rotor-stator spinning disk reactor has also been designed by van der Schaaf and co-workers. This conceptually new photochemical reactor was used in the photocatalytic oxidation of  $\alpha$ -terpinene **92** to the drug ascaridole **93** with rose bengal as photocatalyst (Scheme 20). Throughputs of over 1 kg per day ( $270 \text{ mmol h}^{-1}$ ) were materialised under visible light irradiation. The performance of the reactor directly correlates to various process parameters. Several optimization studies were conducted whereby the authors



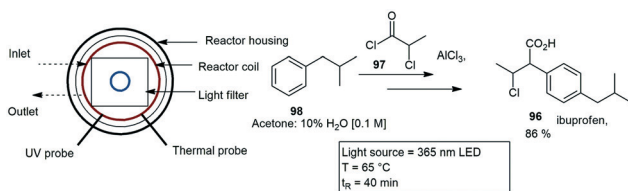
Scheme 20 Rotor stator spinning disk reactor. Photograph reproduced with permission.<sup>75</sup>



investigated: rotation speed, liquid flow rate, and catalyst concentration. The conversion and selectivity of the product increased from 37 to 97% and 75 to 90% respectively. This was achieved with an increase of rotation speed from 100 to 2000 RPM. The authors found that the mass transfer was directly related to the rotation speed of the disk and that the reactor operates with negligible pressure drop and allows for facile fine-tuning of the mixing efficiency.<sup>75</sup>

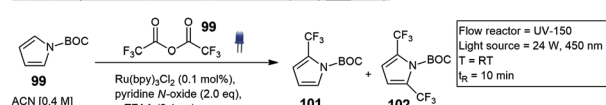
**2.5 Commercial flow photoreactors.** Commercially available flow photochemical reactors are expanding, with companies such as ThalesNano Inc., Vapourtec Ltd, UniQsis Ltd. and many more now offering photochemistry reactor modules. These companies have all developed their own photochemical reactors, and applications expand from research and development to large scale production. The UV-150 photochemical photoreactor from Vapourtec Ltd., has been cited in more than 60 peer reviewed publications and has been used in a variety of chemical transformations. The UV-150 is comprised of a coil reactor comprised of a single layer of thin-walled fluoropolymer tubing mounted inside a sealed reactor housing, the light source and filter (low or high pressure mercury lamps) is then mounted in the middle of the coil reactor. The system can alternatively be configured with standard or high-power LEDs. Several advantages are highlighted by the UV-150 photoreactor including selective temperature control from  $-20$ – $80$  °C, accessible scale-up allowing multiple gram per hour quantities of material being produced, easily changed reactors available in 2 mL, mL and 10 mL volumes, real time spectra data allowing spectral intensity, wavelengths and reactant adsorption to be measured, as well as complete safety with an enclosed light source. The system can alternatively be configured with standard or high-power LEDs.<sup>76</sup> One of the first papers published demonstrating the ability of the UV-150 photochemical photoreactor was by Baumann and Baxendale proceeding with the synthesis of ibuprofen **96** in a photo-Favorskii rearrangement reaction between  $\alpha$ -chloropropiophenone **97** and isobutylbenzene **98**. Various parameters were screened and optimized, it was found that ibuprofen **96** could be prepared in a yield of 86% and a productivity rate of  $1.29$  mmol h<sup>-1</sup>. at a temperature of  $65$  °C with a residence time of 40 min (Scheme 21).<sup>77</sup> Several more reactions, specifically performed with the UV-150 photochemical photoreactor have been highlighted below.

Beatty and co-workers described trifluoromethylation reactions. Trifluoroacetic anhydride **99** and pyridine-*N*-oxide

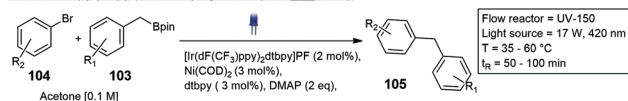


**Scheme 21** The synthesis of ibuprofen under photochemical flow chemistry using a Vapourtec UV-150 reactor.

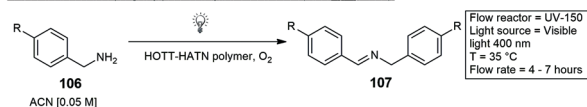
Trifluoromethylations under continuous flow conditions (Beatty *et al.* 2015):



Photoredox C(sp<sup>2</sup>)-C(sp<sup>3</sup>) cross-couplings in flow (Lima *et al.* 2016):

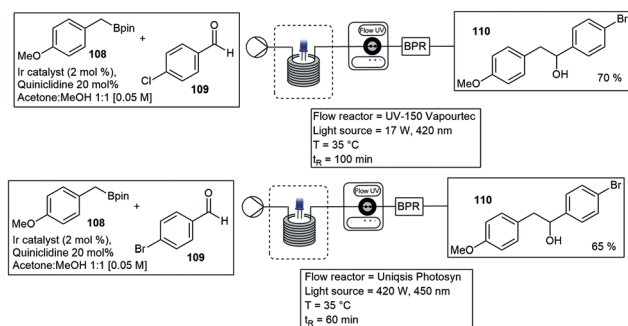


Aerobic oxidative couplings by photocatalytic HOTT-HATN (Xiao *et al.* 2017):



**Scheme 22** Reactions demonstrated on a commercial Vapourtec E-series photo reactor.

was used to trifluoromethylate several arene substrates containing both electron-donating and mildly electron-withdrawing groups. The trifluoromethylation of *N*-Boc pyrrole **100** to the mono- **101** and di-substituted **102** derivatives were achieved in moderate yields (Scheme 22).<sup>78</sup> Decarboxylative C(sp<sup>3</sup>)-C(sp<sup>3</sup>) cross-coupling reactions utilizing dual photoredox iridium-nickel photocatalysts have been reported by Abdiaj and co-workers, Robinson and co-workers and Lima and co-workers.<sup>79–81</sup> In another paper Abdiaj and co-workers developed a method to perform a dual iridium-nickel catalyzed C(sp<sup>2</sup>)-C(sp<sup>3</sup>) cross-coupling reaction by circumventing solubility issues associated with potassium trifluoroborate salts. The formation of an intermediate, with a pyridine-derived Lewis base was found to be essential for the photoredox activation of the boronic esters **103**. Based on these results they were able to develop a further simplified visible light mediated cross-coupling method using boronic esters **103** and various bromo heteroarenes **104** under flow conditions with a residence time of 50 min, blue LED's and  $35$  °C, 50–95% yield was reported for the coupled products **105** (Scheme 22).<sup>82</sup> The UV-150 photochemical photoreactor has also been employed in the aerobic oxidative coupling of benzylamines **106** to enamine **107**, photocatalysed by a novel HOTT-HATN polymer photocatalyst (Scheme 22). In a separate paper the same



**Scheme 23** Commercial application of a photochemical cross-coupling reaction from batch to flow on both a Vapourtec UV-150 reactor and a UniQsis Photosyn reactor.



authors also described arene alkylations in dimethylsulfoxide (DMSO) with a different organic photocatalyst (4-CzIPN) and purple LED's. Reactions proceeded with a residence time of 70 min and yields from 60% (Scheme 23).<sup>83,84</sup> Several more organic catalysts have been designed and implemented in the UV-150 photochemical photoreactor.<sup>85</sup> Several reactions ranging from photoactivated oxadiazolidones,<sup>86</sup> Vilsmeier Haack reactions,<sup>87</sup> Negishi cross couplings,<sup>88</sup> iron-catalyzed Kumada–Corriu cross couplings<sup>89</sup> and several more have been reported with Vapourtec UV-150 photochemical photoreactor. Ley and co-workers published a paper demonstrating both the Vapourtec E-series as well as a prototype UV-reactor from Uniqsis. The reactions that were investigated included the photochemical cross-coupling between boronic esters **108** and carbonyl compounds **109** resulting in the formation of 51 different coupled reactions of which 13 were heterocycles. Reactions were first tested using the Vapourtec UV-150 fitted with a blue LED module 17 W and a 10 mL FEP coil, equating to a residence time of 100 min, a 100% conversion and 70% isolated yield of **110** was obtained. A large scale experiment was carried out using a Uniqsis Photosyn reactor, which operates on a similar principle but is equipped with a more powerful 420 lamp and a bigger 20 mL PFA coil, the residence time was reduced to 60 min and a 65% isolated yield of **110** was produced (Scheme 23).<sup>90</sup>

### 3 Flow electrochemistry concepts

Limitations in conventional electrosynthesis can be overcome when using flow electrochemical devices. A literature overview found that under batch conditions, electrolysis is largely based on performing reactions in a glass beaker with counter electrodes and an electrolyte solution. These reactions are largely equated with a poor performance and a very slow rate of conversion. This has changed with continuous flow electrolysis, which is participating in the trend towards innovative reactor designs in flow cells making selective syntheses with high conversions possible in a single pass through the cell. Continuous flow electrochemistry lends itself to improved mixing, the small gap between electrodes is of particular benefit enhancing high mass transfer and the electrode's surface/volume ratio which in-turn reduces energy consumption, fast heat exchange, multistep reaction sequences, improved reaction selectivity, high reproducibility and reliable scale up, with most of these being unattainable under batch conditions. In-addition the electrodes can easily be replaced by another metal electrode.<sup>8</sup>

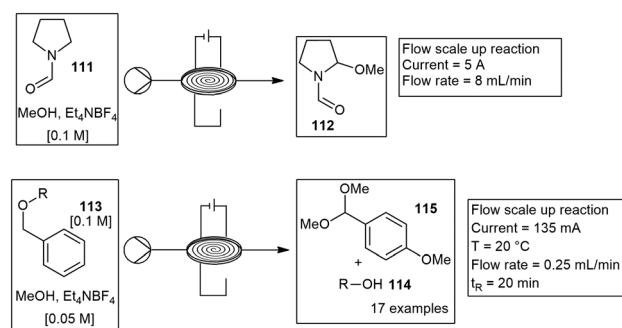
**3.1 Spiral electrochemical flow cell.** Spiral microchannels utilizes a curved microchannel which induces a chaotic advection and enhances the mixing process. The curved microchannels have been shown to be more efficient in comparison to a straight microchannel, mixing wise.<sup>91</sup> Robert Green and co-workers designed a spiral electrolysis cell with a carbon/polymer anode plate and a SS cathode plate with a spiral groove designed for multigram reaction scale. The

circular electrodes were constructed with a diameter of 149 mm and a spiral electrolyte flow channel that was 2000 mm long, 5 mm wide, and had a 0.5 mm interelectrode gap. They demonstrated the efficiency of the cell through a model reaction, the methoxylation of *N*-formylpyrrolidine **111**, achieving a 100% conversion in a single pass with a production rate of 20 g h<sup>-1</sup>. The reaction conditions were carried out at a concentration of 0.1 M *N*-formylpyrrolidine **111** in MeOH with 0.05 M tetraethylammonium tetrafluoroborate (Et<sub>4</sub>NBF<sub>4</sub>), 24 g of the product **112** was obtained in 87% yield at 8 mL min<sup>-1</sup> and a current of 5 A.<sup>92</sup> This electrolytic flow cell was further used in the electrochemical deprotection of *p*-methoxybenzyl (PMB) **113** ethers in MeOH, leading to the unmasked alcohol **114** and *p*-methoxybenzaldehyde dimethylacetal **115** as by-product. The electrochemical method removed the need for a chemical oxidants, and the added electrolyte Et<sub>4</sub>NBF<sub>4</sub> could be recovered and reused. The method was applied to 17 substrates with high conversions in a single pass, with yields of up to 93% and productivities of up to 7.5 g h<sup>-1</sup> being obtained (Scheme 24).<sup>93</sup>

### 3.2 Microchip/channel electrochemical flow cell.

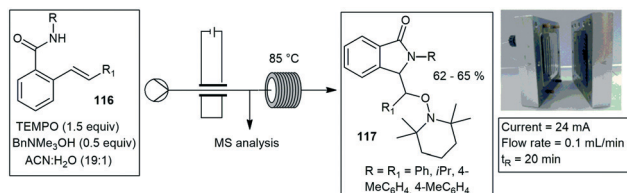
Microchannel electrochemical cells are the easiest and most prevalent electrochemical reactor designs with various examples being reported. Wirth and co-workers printed an electrochemical flow cell reactor with a 3 mm channel width, a 250 μm thickness and a volume of 250 μL, enabling more efficient processing with little or no supporting electrolyte needed, this was demonstrated by the facile synthesis of amidyl radicals used in intramolecular cyclization of amides **116** to produce the corresponding isoindolinones **117**. Various substrates were investigated with yields ranging from 18–96% (Scheme 25).<sup>94</sup>

A similar flow cell was reported by Huang and co-workers demonstrating the synthesis of benzofused S-heterocycles as well as scale-up reactions of these procedures. The custom-built electrochemical flow cell was equipped with a Pt-cathode and an anode made of carbon filled polyvinylidene difluoride (PVDF). The electrochemical cell was manufactured using magnetron sputtering. This method deposits a thin layer of titanium (6 nm) and platinum (200 nm) on a SS plate. The Pt electrode, in turn, was stabilized

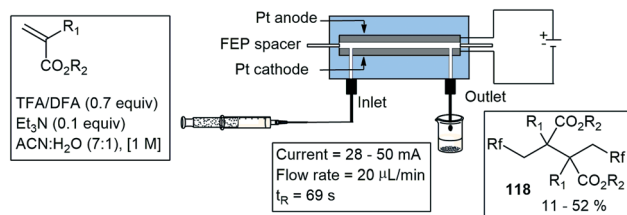


**Scheme 24** Electrochemical synthesis carried out in MeOH in a spiral electrochemical reactor.





**Scheme 25** An easy to machine electrochemical microchannel flow cell used to demonstrate the synthesis of various isoindolinones. Photograph reproduced with permission.<sup>96</sup>



**Scheme 26** Electrolysis of olefins using a single channel electrochemical reactor.

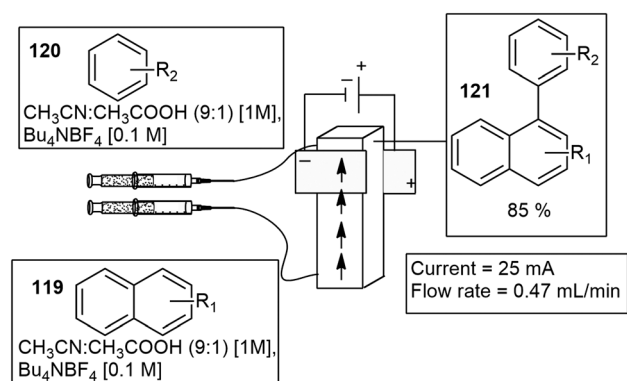
with titanium, increasing the stability and overall effectiveness of the cell. A range of 1,4-benzoxathins and 1,4-benzothiazines were synthesized in moderate to excellent yields. A flow rate of  $0.3 \text{ mL min}^{-1}$  was used which equated to a residence time of 33 minutes, with a current of 35 mA.<sup>95</sup>

Arai and co-workers have designed an electrochemical flow reactor with platinum foil as both the anode and cathode. These were placed on either side of a FEP channel as shown in Scheme 25. The cell consisted of a single inlet and a single outlet, and with this they demonstrated several di- and trifluoromethylation reactions. The transformation of several acrylates **118** were reported with moderate yields (Scheme 26).<sup>96</sup> A year later Arai and co-workers published another electrochemical flow cell with two inlets and a single outlet. The reactor was constructed from glass plates and two platinum Pt electrodes (3 cm width, 3 cm length each). A slit was provided on the cathode plate for introducing the

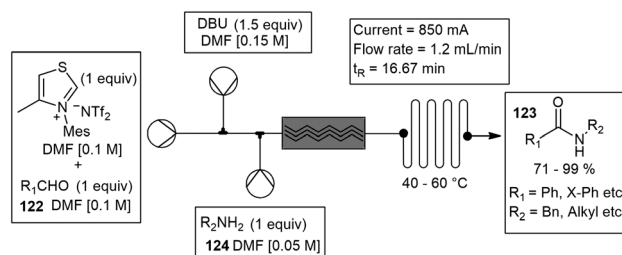
nucleophilic solution into the reactor. They demonstrated an efficient anodic cross-coupling reaction using parallel laminar flow. The model reaction studied proceeded effectively in single flow through operation and the desired product was obtained in much higher yields compared to the performance in a conventional batch cell. Naphthalene **119** was coupled with an alkylbenzyl substrate **120**, forming **121** in 85% yield at a rate of  $0.47 \text{ mL min}^{-1}$  (Scheme 27).<sup>97</sup> This work was similar to that demonstrated by Kuleshova who designed a single channel electrolysis flow cell in 2012 and applied it to the methoxylation of *N*-formylpyrrolidine in high conversion.<sup>98</sup>

Robert Green and co-workers developed a similar flow cell constructed from two rectangular electrode plates ( $53 \text{ mm} \times 40 \text{ mm} \times 2 \text{ mm}$ ). The working electrode was constructed with a carbon PVDF blend, and the counter electrode from SS. They described the oxidative conversion of aldehydes **122** to amides **123** mediated through *N*-heterocyclic carbenes (NHC). This was achieved through the oxidation of Breslow intermediates. After electrochemical oxidation, the reaction intermediate is completed by passage through a heating cell. The flow mixing regimen circumvented the issue of competing imine formation between the aldehyde **122** and amine substrates **124**, which otherwise prevented formation of the desired product **123**. High yields (71–99%), productivities (up to  $2.6 \text{ g h}^{-1}$ ), and current efficiencies (65–91%) were realized for 19 amides (Scheme 28).<sup>99,100</sup> Noël and co-workers have designed a modular and scalable electrochemical flow reactor consisting of an undivided electrochemical cell with a flexible reactor volume (Scheme 29). Their reactor was designed to be used in two different modes: either serial (with volumes ranging from 88  $\mu\text{L}$  to 704  $\mu\text{L}$ ), or a parallel mode (numbering up). The electrochemical oxidation of sulfides were studied with the transformation to either sulfoxide or sulfone. Residence time applied voltage and microchannel thickness was studied with an optimal yield of 98% for the desired products. Reaction conditions concluded with a residence time of 10 min and an applied voltage of 2.8 V. Furthermore, the aziridination of alkenes with primary amines using the same electrochemical microreactor with yields ranging from 19–94%, was also studied.<sup>101,102</sup>

**3.3 Commercial electrochemical flow cells.** The first commercially available electrochemical flow reactor was

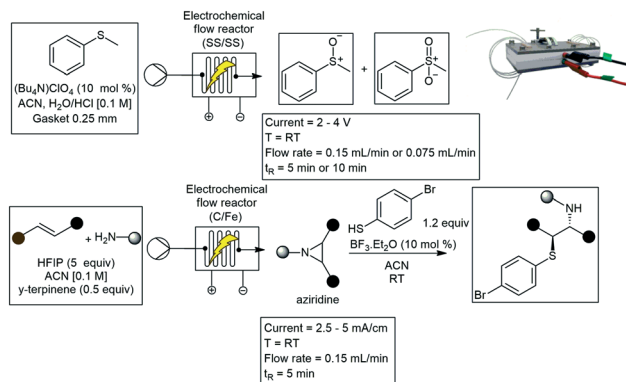


**Scheme 27** Anodic C-C cross coupling with naphthalene and a custom built electrochemical flow cell.

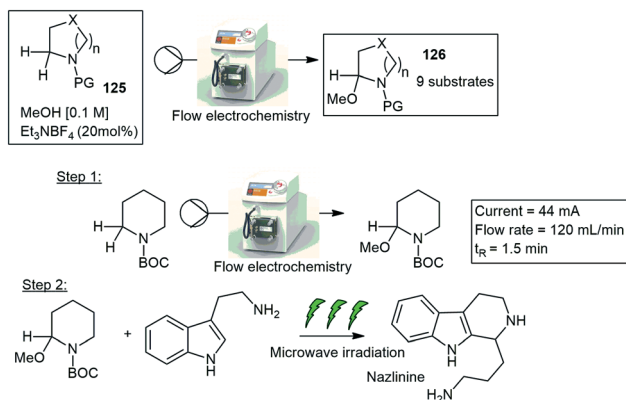


**Scheme 28** An electrochemical microreactor designed to produce amides from aldehydes through a Breslow intermediate.





**Scheme 29** A modular and scalable electrochemical flow reactor consisting of an undivided electrochemical cell with a flexible reactor volume. Photograph reproduced with permission.<sup>101</sup>



**Scheme 30** Syrris Asia electrochemical reactor showing the production of nazlinine.



**Fig. 2** Commercial electrochemical reactors.

produced by Syrris Asia Ltd., the methoxylation of indole derivatives **125** was demonstrated under flow conditions to produce the methoxylated products **126**. They further expanded their focus to prepare nazlinine **127** in 59% yield over two steps, with the first step being an electrochemical oxidation and the second step a microwave irradiation. The protected piperidine moiety **128** was oxidised to form the methoxylated counterpart **129**, which was treated with triptamine **130** under microwave conditions to form nazlinine **127**. The electrochemical oxidation proceeded in MeOH (0.1 M) with 20 mol% electrolyte. Nine substrates were produced at a rate of 120  $\mu\text{L min}^{-1}$  with yields above 90% (Scheme 30, Fig. 2).<sup>103</sup>

A recent piece of equipment from Vapourtec Ltd., the ion electrochemical flow reactor (Fig. 2), has been used to demonstrate the formation of hypervalent iodine reagents by Elsherbini and co-workers. The reactor (reactor volume = 0.6 mL, spacer 0.5 mm) is fitted with a glassy carbon anode and a platinum cathode. The use of electricity replaces hazardous and costly chemical oxidants generally associated with these types of transformations. Various substrates were oxidised in relatively high yields.<sup>104</sup> Furthermore using the same ion electrochemical setup Amri and co-workers demonstrated the efficient mono- and dialkoxylation of pyrrolidine-1-carbaldehyde, with precise control of the reaction conditions either the mono- or the dialkoxyated products were formed.<sup>105</sup>

Cambridge reactor design (CRD) and Uniqsis supply the Ammonite 8 and 15 electrochemical flow reactors (Fig. 2) which are comprised of a clamshell type channel reactor with a spiral flow path (2 mm  $\times$  1.0/0.5 mm) which is designed to maximise the path length/size ratio of the system.<sup>104</sup>

#### 4 Multiphase chemistry under flow conditions

Several approaches to gas–liquid flow reactions have been studied, most of these involved the use of a biphasic flow regime. In the case of gas–liquid reactions, a high interfacial area is essential for an efficient mass transfer rate. Batch reactions performed in a traditional round bottomed flask have much lower interfacial areas, and this decreases with an increase in the size of the flask. The exact flow regime depends on the gas and liquid flow rates, channel pattern and dimensions, and the physical properties of the fluid and gas composition. The flow regimes observed include segmented flow, bubble flow, stratified flow and annular flow (Fig. 3). Under microfluidic conditions segmented flow, described as bubbles of gas that are separated by slugs of liquid dominates. In contrast annular flow involves a gas and liquid stream concurrently flowing together, arising when a fast flowing high pressured gas stream is introduced into a liquid stream at lower pressures pushing the liquid against the microchannel wall.<sup>106</sup> Most gas–liquid reactions in flow chemistry follow a segmented flow regime coupled with a mass flow controller (MFC) to accurately dose the amount of gas into the flow stream, gases utilised include carbon

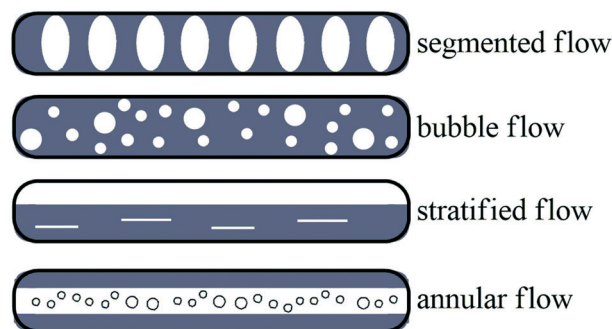
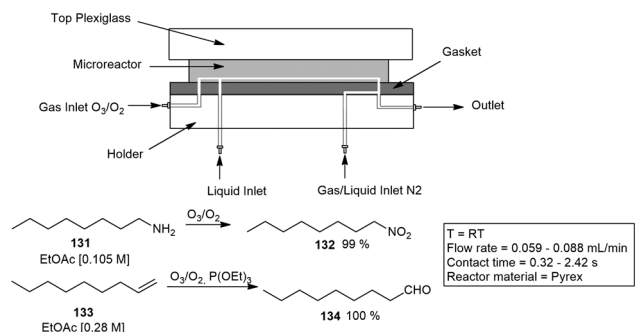


**Fig. 3** Flow regimes.



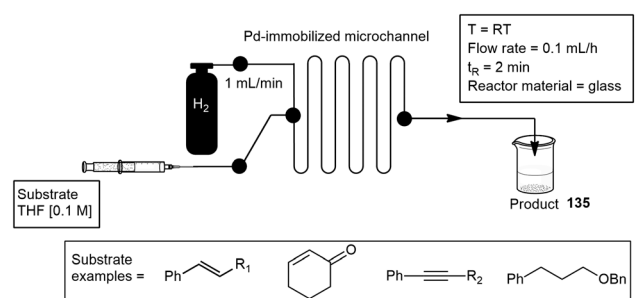


**Scheme 31** Ozonolysis reactions using a silicon Pyrex microreactor.

dioxide,<sup>107</sup> oxygen,<sup>108</sup> nitrogen,<sup>109</sup> hydrogen sulphide,<sup>110</sup> hydrogen, carbon monoxide<sup>111</sup> and ethylene gas.<sup>112</sup>

**4.1 Static mixers and microchannels for a biphasic flow devices.** Jensen and co-workers were one of the first groups to report ozonolysis reactions under continuous flow conditions and they established this with a multichannel microreactor designed and fabricated using silicon and Pyrex. They included microfabricated silicon posts in the channels as a means to increase mass transfer between the gas and liquid phase, the multichannel reactor consisted of 16 individual reaction channels (600  $\mu\text{m}$  wide  $\times$  300  $\mu\text{m}$  deep, 22.7 mm long). With this device they investigated the ozonolysis of octylamine **131** to the nitro derivative **132** as well as the ozonolysis of 1-decene **133** to the equivalent aldehyde **134**, in both reactions 99–100% conversion was observed (Scheme 31).<sup>113</sup>

Kappe and co-workers printed a SS reactor by selective laser melting. The reactor was designed specifically for difluoromethylation reactions with fluoroform gas and *n*-BuLi. The reactor was constructed from SS with a 0.8 mm ID and 2.4 m OD. The reaction channel was designed with a slight oval cross section. The specific geometry allowed improved surface quality on the top surface of the reaction channel by reducing the printing area that overhangs into the metal powder. Reactions were performed at  $-65\text{ }^\circ\text{C}$  and 2 min residence time. A 0.5 M solution of diphenylacetoneitrile in THF was pumped at a flow rate of  $0.8\text{ mL min}^{-1}$ , the *n*-BuLi was fed into the system at rate of  $0.36\text{ mL min}^{-1}$ , a 50 s residence time was obtained in the first zone which was combined with the fluoroform gas at a rate of  $26.7\text{ mL min}^{-1}$ .



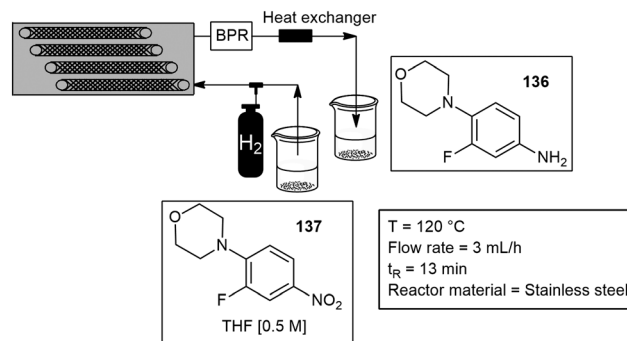
**Scheme 32** Immobilized palladium catalyst in a microchannel custom built for hydrogenation reactions.

The residence time in the second zone was 1 min, an overall yield of 81% was achieved with a production rate of  $79\text{ mg min}^{-1}$ .<sup>114</sup>

One of the first microchannel reactors plated with an immobilized catalyst was developed by Kobayashi and co-workers in 2003. They conducted several alkene hydrogenations and debenzylations, which proceeded efficiently to afford the desired products **135** in a quantitative yield within 2 minutes. They selected a microchannel reactor having a 200  $\mu\text{m}$  channel width, 100  $\mu\text{m}$  channel depth, and a length of 45 cm. They immobilized a Pd catalyst on the wall of the glass channel with a cross linking polymer. Yields of up to 97% were obtained (Scheme 32).<sup>115</sup>

Bendova and co-workers custom built a microfluidic chip for a stereoselective hydrogenation reaction. The microchip consisted of two main inlet ports, a static mixer followed by a residence time loop, a third inlet port for a quencher, a second static mixer, and an outlet port. The total volume was 10  $\mu\text{L}/19.5\text{ }\mu\text{L}$ , and provided residence times from 15–120 s for flow rates in the range from 5–20  $\mu\text{L min}^{-1}$ . The reactor was used to transform methylacetoacetate (MAA) to (*R*)-methylhydroxybutyrate in an ionic liquid  $[\text{Tf}_2\text{N}]/\text{MeOH}/\text{H}_2\text{O}$  phase, with great success at conversions above 97%. They further used the same microfluidic chip reactor to design the reversible biphasic arrangement for asymmetric hydrogenations of MAA.<sup>116</sup>

Tsanaktsidis and co-workers custom built a catalytic static mixer (CSM), for the synthesis of a key intermediate of the antimicrobial drug linezolid (Zyvox). The approach combined three-dimensional (3D) printing and additive manufacturing techniques. They obtained a general method for catalytic hydrogenations and the rapid production of **136** from the nitro substrate **137** without the need for catalyst removal or recovery, the reaction productivity proceeded with  $317\text{ g L}^{-1}\text{ h}^{-1}$ . The CSM's consisted of metal inserts (150 mm  $\times$  6 mm), designed for optimal mixing, onto which the metallic catalyst was deposited using an axial flow cell and standard electroplating techniques. The tubular flow reactor itself is approximately the size of a loaf of bread and contains a set of 12 CSM's that were simply and easily inserted into the tubular reactor and operated in series inside the



**Scheme 33** Static mixers for the hydrogenation of a nitro group to an amine.



temperature-controlled housing. The reactor volume was approximately 39 mL, and a hydrogen gas line was attached at the front end of the reactor to facilitate gas-liquid mixing with the substrate (Scheme 33).<sup>117</sup> They later reported another paper with the same 3D printed CSM, however in this paper the CSM was plated with either palladium or nickel catalyst, and the system was tested on the reductive amination of aldehydes and ketones to amides with moderate to excellent yields.<sup>118</sup> Several static mixers have been reported under flow conditions for more details see.<sup>118–121</sup>

#### 4.2 Membrane microreactors for gas-liquid applications

**Microchannel membrane reactors.** Kim and co-workers have developed multiple dual and triple channel photoreactors.<sup>122,123</sup> The first microreactor consisted of two microfluidic channels separated by a thin PDMS semipermeable membrane, allowing the diffusion of gases from the gas channel into the liquid phase (Scheme 32). They first demonstrated an oxidative Heck reaction making use of arylboronic acids **138** and simple alkenes **139**. The products **140** were produced in yields ranging from 75–82%. A year later they published a second reactor model with a triple channel system. The reactor was used for the photosensitized oxygenation of (–)-citronellol **141** to **142** and **143**, the microfluidic channels were again separated by the thin PDMS membrane (Scheme 34). Oxygen was introduced in one channel and transported through the membrane towards the liquid channel. The latter channel was irradiated with a white LED light source. Several other membrane reactors with immobilized catalysts have also been developed.<sup>124,125</sup>

**Tube-in-tube microreactors.** The pioneering work by Steven Ley's group demonstrated the first tube-in-tube reactor, designed to deliver gaseous substance into a continuous flowing stream. The first papers were published between 2010 and 2011, demonstrating the tube-in-tube reactor with AF-

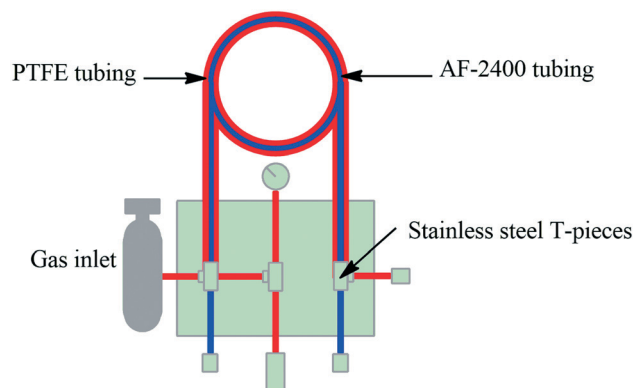
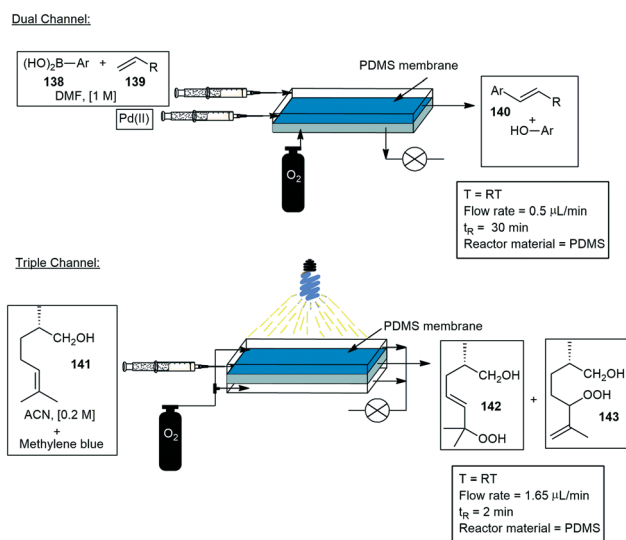


Fig. 4 Semipermeable tube-in-tube reactor for gaseous addition to a continuous flowing stream.

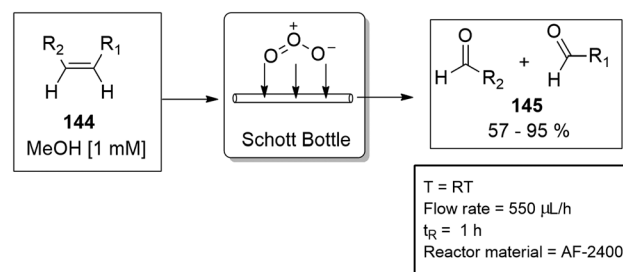
2400 tubing, a semipermeable tubing allowing the diffusion of gasses into a continual flowing stream. The Teflon AF-2400 tubing was placed within the 1/8" OD, PTFE tube. This configuration allowed the flow of a substrate stream within the membrane tubing whilst the gas filled the PTFE outer tubing and diffusion transfers the reactive gas into the substrate stream. The Teflon AF-2400 (1.0 m, 0.28 mL) and the outer PTFE tubing was separated by SS T-pieces (Fig. 4).<sup>34,126,127</sup> With this they demonstrated the carboxylation of Grignard reagents under flow conditions. Several more papers have since been published demonstrating this technology.<sup>12,126,128–132</sup> Uniqsis Ltd. and Vapourtec Ltd. have also adapted this technology for commercial tube-in-tube reactors.

Before the innovative design of the tube-in-tube gas module, Steven Ley's group demonstrated the principle with a continuous flow ozonolysis reaction. The semi-permeable Teflon AF-2400 tubing was coiled inside a standard Schott bottle and pressurised with ozone gas. The liquid stream was saturated with ozone gas by means of diffusion. The concept was proven successful by demonstrating the ozonolysis reaction on 11 different alkenes **144** with yields ranging from 57–95% for the equivalent aldehydes and ketones **145** (Scheme 35).<sup>130</sup>

**Falling film reactor.** The falling film reactor is based on a liquid film forming due to a liquid feed falling under gravity against a solid microstructured surface. The gas phase then flows co-currently or counter-currently in front of the liquid

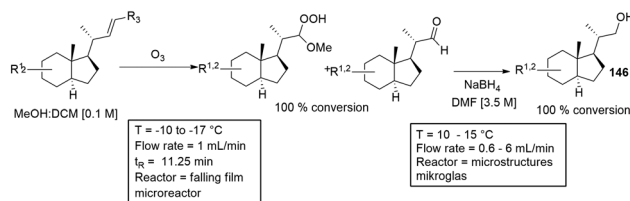


Scheme 34 A PDMS membrane reactor used in a basic Heck reaction as well as the photocatalytic oxygenation of (–)-citronellol.



Scheme 35 The ozonolysis of various alkenes using AF-2400 semipermeable tubing.

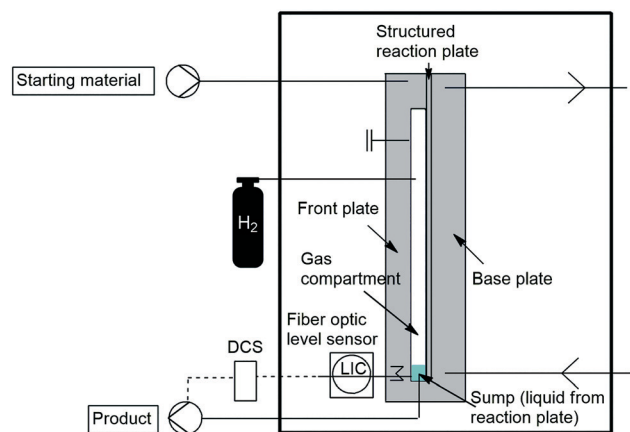




**Scheme 36** Vitamin D analogue preparation *via* ozonolysis in flow.

phase. The principle of falling film microreactors have been adapted and utilized by several flow chemistry research groups over the past few years. Recently Chen and co-workers<sup>133</sup> designed a novel double-side falling film microchannel contactor, and investigated the absorption coefficient of carbon dioxide in water. A similar design was shown by Steinfeldt and co-workers<sup>134</sup> investigating the cyanide degradation *via* ozone absorption as well carbon dioxide absorption. The reaction plate was fabricated with 64 microchannels of 100 mm (length), 0.9 mm (width) and 0.5 (depth). The wall separating the channels had a width of 1 mm. Janisch and workers designed a practical falling film reactor, successfully synthesizing the important intermediates of vitamin D analogues **146**. The reaction sequence consisted of an ozonolysis step and a subsequent reduction (Scheme 36).

Recently Rehm and co-workers demonstrated the value of falling film reactors in a photocatalytic application by applying external irradiation to the falling film microreactor. The reactor consisted of a back plate carrying a heat exchanger, as well as an inlet and outlet for the reaction solution which is fed through the falling film by gravity. A front plate with an inspection window constructed out of borosilicate glass and a middle plate (the reaction plate) constructed of microchannels with different geometries. LED's were installed and connected to cover the front inspection window. The microstructured falling film reactor was applied to the dye-sensitized photochemical conversion of 1,5-dihydroxynaphthalene to juglone.<sup>135</sup> Several examples



**Scheme 37** Microwave transparent catalytic falling-film microreactor for automated operation.

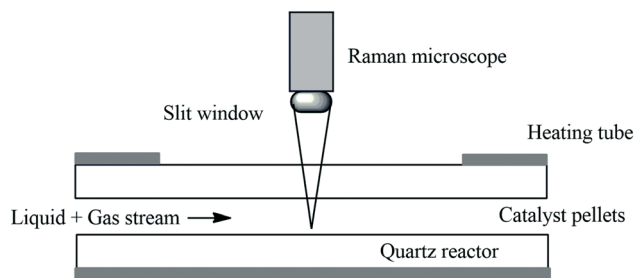


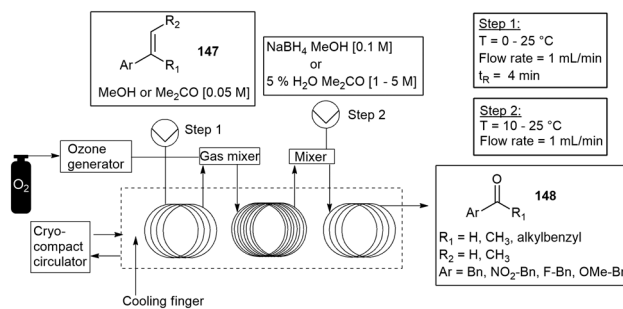
**Fig. 5** Solid phase quartz reactor design for triphasic reactions.

of photocatalytic falling film reactors have since been developed and reported on.<sup>136–138</sup>

In 2018 Krtuschil and co-workers developed a falling film microreactor to study heterogeneously catalysed gas–liquid reactions under MW irradiation. They developed a fully automated pilot scale procedure for semi-hydrogenations. The microchannels of the reaction plate were coated with a novel selective catalyst. A special fibre-optical sensor was also developed to control the liquid level in the sump of the microwave reactor. With this they demonstrated the semi-hydrogenation of triple bonds to double bonds, avoiding over-reduction to single bonds (Scheme 37).<sup>139</sup>

**4.3 Unconventional devices.** A 350 °C fixed-bed multiphase reactor was designed by Duarte and co-workers to perform gas–liquid–solid reactions. The reactor was composed of a cylindrical shaped quartz reactor encased in a Joule effect SS tube as shown in Fig. 5. Millimetric sized heterogeneous catalyst pellets were inserted in the centre of the cylindrical tube. A gas–liquid flow stream was then allowed to flow through the reactor. They validated the reactor, along with the acquisition of Raman spectra (made possible through the incorporation of a slit window in the SS heating tube) by performing diesel hydrodesulfurization on a CoMo/alumina extruded catalyst.<sup>140</sup>

Wenn and co-workers have used a mesh microreactor design to introduce a gas and liquid flow stream. Reactor enclosures defining chambers on each side of the mesh were formed from milled glass and metal components. They validated their reactor design by performing the hydrolysis of colourless fluorescein diacetate in toluene. Micromeshes with



**Scheme 38** The ozonolysis of various aromatic alkenes with the ThalesNano O-Cube.

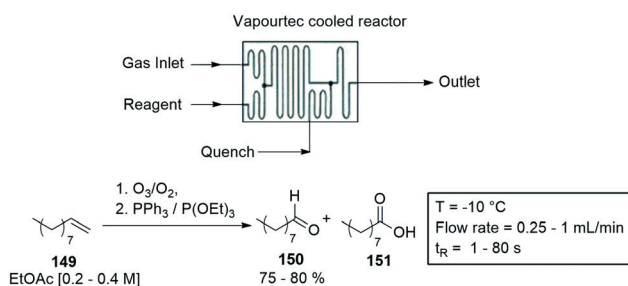


a pore diameter, depth, and spacing each of 5  $\mu\text{m}$  were formed by electrodeposition.<sup>141</sup>

**4.4 Commercial reactors.** Flow companies such as ThalesNano Inc., Uniqsis Inc. and Vapourtec Inc. have all fabricated their own gas–liquid–solid commercial reactors. In 2010 Oliver Kappe and co-workers performed both an ozonolysis step and quenching step under continuous flow conditions using the O-Cube by ThalesNano Inc (Scheme 38). Various aromatic alkenes **147** with different quenching reagents were tested. They obtained isolated yields between 72–90% for their selected products **148**.<sup>142</sup> The O-Cube consists of a channel with PTFE tubing of variable lengths, embodied in a metallic plate fixed on a Peltier plate. The starting/quenching materials were delivered continuously into the temperature-controlled reaction zones by the pumps and the product is collected in the end in a vial, flask or vessel.

The pioneering work of Steven Ley and co-workers set the bar for commercial tube-in-tube reactors which has been quickly adapted by commercial flow companies. Uniqsis Inc. has named their tube-in-tube reactor the gas addition module (GAM), also constructed with AF-2400 tubing, the gas stream and the liquid flow stream flowed in opposite directions, with the gas phase in the inner tube and the liquid in the surrounding tube. Kappe and co-workers identified the GAM as a potential tool to perform safe and scalable gaseous reactions with hazardous diazomethane gas. They performed various reactions which included methylations of various nucleophiles; [2,3]-cycloadditions and cyclopropanation of alkenes. Yields ranging from 59–99% were reported. Brzozowski and co-workers covered an extensive review on various reactions performed under continuous flow conditions with the GAM as well as AF-2400 tube-in-tube reactors.<sup>12</sup>

Vapourtec Inc. has also launched their version of the tube-in-tube reactor fabricated with AF-2400 tubing. The gas–liquid reactor fits into the standard glass manifold and is seen to be compatible with all existing R-Series systems. The liquid phase is fed through a coil, with a connection for the gas phase pressure from a regulated supply. Huvaere and co-workers developed a method to perform photooxidations and they validated the reactions using a model system, the photooxidation of ethyl 3-(2-furyl)propanoate. The reaction was further optimized for optimal conversion.<sup>56</sup>



**Scheme 39** Ozonolysis of alkenes using a commercially available Vapourtec cooled reactor cell.

A second gas–liquid reactor was designed by Vapourtec Inc., a mixed flow cooled reactor module, and its efficiency was demonstrated with the ozonolysis of various alkenes. The gas reactor was coupled with a cooled flow cell to perform the ozonolysis of *n*-decene **149**. The reactions were carried at flow rates of 0.25–1 mL min<sup>-1</sup>, and temperatures of –10 °C. Residence times varied between 1–80 s, with **150** produced in 75–80% yield, and the by-product **151** in 15–20% (Scheme 39).<sup>143</sup>

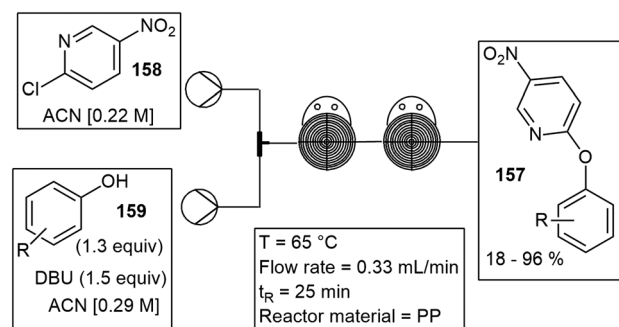
### 5 3D printing in flow chemistry

3D printing, also called additive manufacturing (AM) or rapid prototyping (RP), is a layer-by-layer manufacturing method and has been widely used in many areas such as organ printing, aerospace and industrial design. In this section, we focused on the advances of 3D printed microfluidic chips especially modified for use in continuous flow chemistry. Based on a brief overview of different 3D printing methods and materials, we have chosen to highlight a few papers describing some of these method applications in microfluidics here.<sup>10,144,145</sup>

**5.1 3D printed microchannel flow devices.** Rossi and co-workers fabricated a 3D printed mesoflow reactor from polyacetic acid (PLA), high impact polystyrene (HIPS) and nylon, which was used for a catalytic stereoselective Henry type reaction. Different 3D printed reactors were screened, and the best performing reactor was identified. A two-step reaction to obtain biologically active 1,2-amino alcohols (norephedrine, metamamol and methoxamine) was developed with high selectivity and yields.<sup>146</sup>

Cronin and co-workers designed two custom made flow systems and utilised two types of organic reactions which included an imine synthesis and an imine reduction. Both reactors consisted of two inlets and a single outlet. The approximate volume of the first reactor was 0.4 mL and was employed in the imine syntheses, while the second reactor had a volume of 0.35 mL and was used in the imine reduction processes. Both reactors were fabricated from polypropylene (PP), a thermopolymer that is inert in a range of organic solvents and organic compounds.<sup>144,147</sup>

Hilton and co-workers followed with another PP 3D printed continuous flow module. The reactor module was



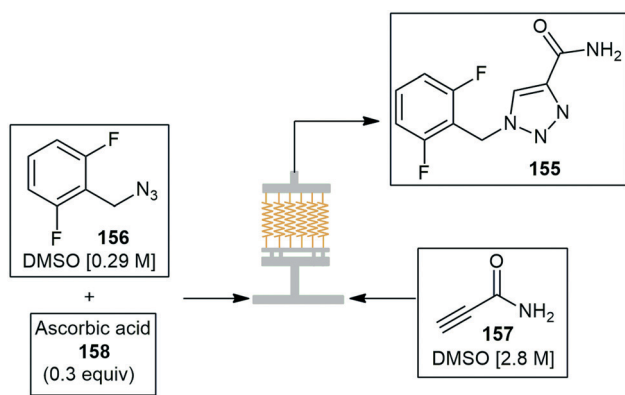
**Scheme 40** Circular disk reactor 3D printed using PP.



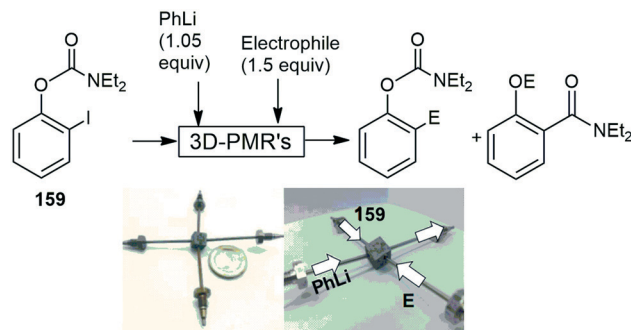
designed as a circular disk reactor CDR to easily fit onto any commercial stirrer plate. The custom-built reactors were 75 mm wide and 7 mm high with an internal 2 mm reactor channel. All of the reactors were printed on an Ultimaker 3, 3D printer using PP filament which resulted in an internal volume of 4.2 mL. The reactor was able to facilitate the formation of a range of ether derivatives **152** from aryl halides **153** and aromatic alcohols **154** with most proceeding with good to excellent yields of the product (Scheme 40). The number of CDR's were increased in series to obtain longer residence times and improved yields, with the flow rate being maintained at  $0.33 \text{ mL min}^{-1}$  and the temperature at  $65 \text{ }^\circ\text{C}$ .<sup>148</sup>

A photoactive monomer was incorporated into a 3D printing resin, which was used to fabricate a 3D photosensitizing flow reactor, which was incorporated in the singlet oxygen synthesis reaction under visible light irradiation. A solution containing 2-furoic acid was pumped together with oxygen through the photoreactor at a flow rate of  $0.1 \text{ mL min}^{-1}$ , irradiated at 420 nm and recycled for 5 h.<sup>149</sup>

Kim and co-workers implemented a numbering-up microreactor system composed of stainless steel and copper was fabricated by CNC machining and 3D printing. The reactor was used in a cost-effective manner in the high throughput synthesis of rufinamide **155**, an anticonvulsant medicine. The reactor consisted of 25 coiled copper capillaries configured in parallel to achieve high throughput experimental studies. Total flow rates of 6, 12, and 24  $\text{mL min}^{-1}$  were tested during the optimization of the azide-alkyne cycloaddition reaction. Reactants 2,6-difluorobenzyl azide **156** and propiolamide **157** were passed through the copper capillary reactor along with ascorbic acid **158** to afford rufinamide **155**. The numbering-up approach allowed the scale-up of rufinamide **155** achieving a high productivity ( $31 \text{ g h}^{-1}$ ) at  $12 \text{ mL min}^{-1}$  flow rate and  $110 \text{ }^\circ\text{C}$ , which equated to roughly 25 times more product than that obtained using a single reactor with the same yield. The main body of the reactor was fabricated by CNC machining and the complex baffle disk as shown in Scheme 41 was fabricated by 3D printing.<sup>150</sup>



**Scheme 41** Copper coiled reactor fabricated by using 3D printing and CNC machining.

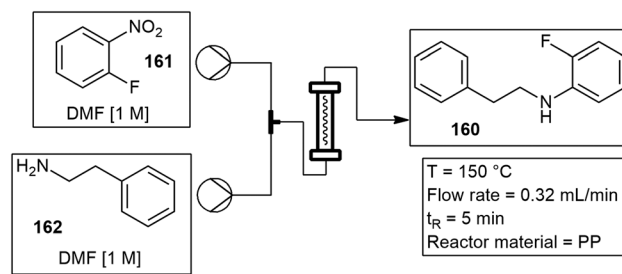


**Scheme 42** 3D-printed stainless steel metal microreactor, utilized in a Fries rearrangement. Photograph reproduced with permission.<sup>151</sup>

The use of 3D-printed stainless-steel metal microreactors (3D-PMR's), have also been gaining interest with the same research group Kim and co-workers fabricating a circular metal reactor with different cross-sectional geometries with the aim to control ultrafast intramolecular rearrangement reactions in a comparative manner. The 3D-PMR with circular channel flow paths demonstrates the improved controllability in rapid Fries-type rearrangement reactions. This is mainly due to the superior mixing efficiency to rectangular cross-section microchannels ( $250 \mu\text{m} \times 125 \mu\text{m}$ ) which has been confirmed based on computational flow dynamic simulations. The high mixing efficiency of **159**, phenyllithium and the appropriate electrophile created by the 3D-PMR's has resulted in high conversions and yields being achieved for the Fries rearranged products with residence times of  $333 \mu\text{s}$  (Scheme 42).<sup>151</sup>

**5.2 Solid phase column reactors.** Hilton and co-workers have also designed and printed a PP mesocolumn reactor. This solid phase reactor was incorporated in the synthesis of heterocycles including the core structure of the natural product ( $\pm$ )- $\gamma$ -lycorane. Several  $\text{S}_{\text{N}}\text{Ar}$  reactions were also investigated with the 3D printed flow reactor. Relatively harsh synthetic conditions were employed initially to explore the limits of the 3D printed PP reactors using polar solvents and high temperatures. Fluoronitrobenzene derivatives **161** were fed together with aryl amines **162** to afford the coupled product **160** at  $150 \text{ }^\circ\text{C}$  and a flow rate of  $0.32 \text{ mL min}^{-1}$  (Scheme 43).<sup>152</sup>

**5.3 3D printed reactor components.** There has been a wide demand for the production of custom-built components, and



**Scheme 43** Solid phase column reactor printed for the synthesis of heterocycles.



this can be seen with many research groups printing their own components. Adamo and co-workers have printed numerous components such as coil reactors, back pressure regulators and many more. An aluminium case was printed for the reactor coils and fitted with 5 mL and 10 mL PFA tubing. The aluminium case surrounding the PFA coil provided a way to extend the use of the tubing to higher temperatures and pressures since the metal takes the mechanical load. Diphenhydramine hydrochloride, lidocaine hydrochloride, diazepam and fluoxetine hydrochloride were all synthesized utilizing these coil reactors.<sup>3</sup>

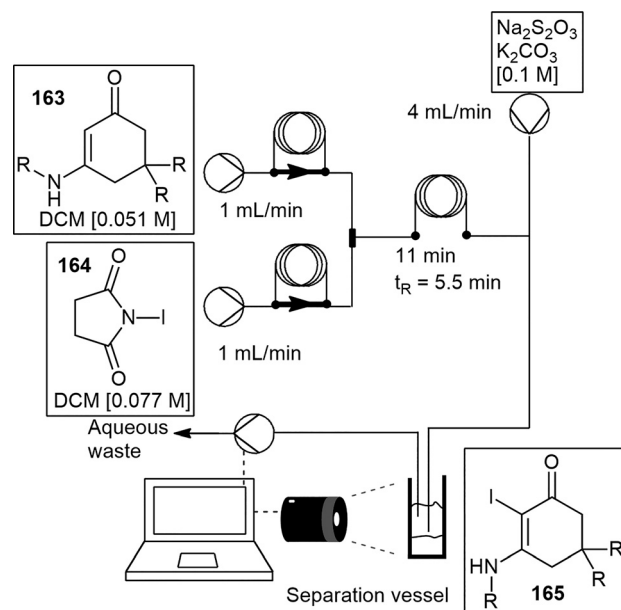
Cronin and co-workers printed a device designed to synthesize supramolecules on microliter scale. Metal-salt coordinating complexes were formed in MeOH. The PP device consisted of 3 inlets and a single outlet which was fed into a T-piece specifically designed to split the stream to collect and separate samples for ESI-MS real time analysis.<sup>147</sup> Similarly Gong and co-workers have printed several microreactor components such as valves, pumps and multiplexers from a specially formulated resin consisting of a monomer, photo initiator and absorber, which allows for longer and more durable use.<sup>153</sup>

## 6 Advanced computer technology

Advanced computer technologies have led to the integration of software and technologies for performing multi-step synthesis under flow conditions. Notable the Ley group have been key players in this field of research with a particular focus on advocating for machine assisted continuous flow chemistry.<sup>154</sup> They have envisioned the many possibilities of this technology and integrated it into synthetic procedures of small organic molecules and API's.

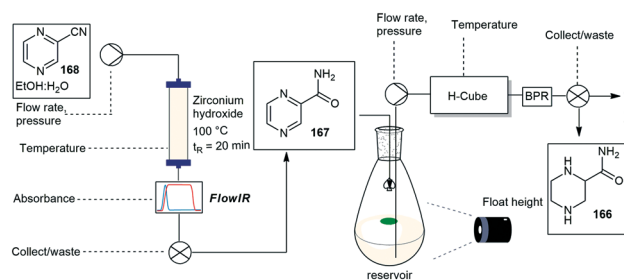
To date there are several reports detailing how computer technologies have been integrated in enhancing the processing of small organic molecules and pharmaceutical compounds in end-to-end multistep processes. These include examples of algorithmic chemical search, whereby a range of reaction types could be accessed and, thus, the flexibility of these single, compact flow designs may be revealed. Another example includes automation of flow systems which allow several reactions to take place on the same system, enabling direct comparison of reactions under different conditions. Moreover, the production of new and known target compounds can be made faster and more efficient, the recipes of which can then be stored as digital files. Some of the automating software has employed machine-powered learning to assist the chemist in developing intelligent algorithms and artificial intelligence (AI) driven synthetic route planning. This ultimately produces a continuous flow platform that can design its own viable pathway to synthesize a particular molecule.

Commonly available software platforms used to control reagents, hardware modules and analytics in a user-friendly manner include MATLAB and LabVIEW. These software's allow remote progress monitoring. Which is also compatible with optimisation algorithms, *e.g.* flexibility and generality.



**Scheme 44** Liquid-liquid separations using computer aided technology.

**6.1 Camera enabled techniques.** The use of video technology has become an integral part of our everyday lives. Recent developments have shown the use of this technology in laboratories. Digital cameras connected to computer vision algorithms have been used to perform some of the activities that take up valuable time, such as work-up operations, sample preparations and continuous data collection.<sup>155</sup> Several research groups have demonstrated camera enabled techniques to aid in visualization, optimizations and performance in chemical reactions.<sup>156,157</sup> O'Brien and co-workers demonstrated a machine assisted in-line liquid-liquid extraction, incorporated in the iodination of enaminone **163**. The enaminone **163** was incorporated with the iodating agent **164** to produce the desired halogenated product **165**, by incorporating an in-line extraction of the organic and aqueous phase. The system was able to cope with significant colouration of the organic reaction stream and with significant volume/flow changes in the aqueous and organic phase streams. A biphasic mixture of the aqueous and organic layer was pumped into a separation vessel. The liquid level was monitored with a webcam, and programmed



**Scheme 45** Automated flow synthesis of piperazine-2-carboxamide.



to pump the aqueous phase out and stop as soon as the level dropped to a certain point (Scheme 44).<sup>158</sup>

**6.2 Automated reaction optimizations.** The use of an open-source software platform was used to synthesize piperazine-2-carboxamide **166** in two steps. The software was used to control and link multiple devices in the flow synthesis.<sup>159</sup> The first step involved the formation of the amide **167** *via* the hydration of nitrile compound **168**. Under the optimized conditions a solution of the nitrile **168** was fed through a column reactor packed with zirconium hydroxide at 100 °C for 20 min, to obtain quantitative yield of the amide **167**. They monitored and controlled the reaction progress using a programmed sequence of operations written with Python. A number of parameters are read from devices or sensors, and the effluent was only collected when all of the parameters were stable, ensuring a high degree of purity in the collected material (Scheme 45). The subsequent reduction reaction was optimized in an autonomous fashion. A two-level factorial design with three parameters (temperature: 40 °C and 100 °C; H<sub>2</sub> pressure: 20 bar and full hydrogen mode; and flow rate: 0.1 mL min<sup>-1</sup> and 0.2 mL min<sup>-1</sup>) were tested in 16 experiments (two repeats each of eight sets of conditions). The two steps were linked by continuously monitoring the reaction reservoir with a camera (Scheme 45). A year later they developed another software system (the LeyLab) that would enable researchers to monitor and control reactions from any internet-connected device. The software was described as a self-optimizing tool to find the best conditions meeting customizable, multicomponent optimization functions. This was demonstrated with an Appel reaction. The software was able to perform 30 experiments, optimal conditions for five experimental parameters were determined in 10 h (temperature, residence time, overall concentration, and equivalents of two reagents relative to a third).<sup>160</sup> They further demonstrated the integration between batch and flow reactors with the automation of downstream processes in the multistep synthesis of 5-methyl-4-propylthiophene-2-carboxylic acid in a telescoped fashion with solvent extractions and solvent swapping techniques.<sup>161</sup>

They further harnessed the power of the cloud and remote servers to demonstrate the synthesis of tramadol, lidocaine and bupropion in a sine automated fashion from across the world.<sup>162</sup> This automated control system was shown to be unencumbered by location or time domain. The control system had facilitated the rapid transition from an unexplored route to an optimized and telescoped process within four working days. Bupropion was synthesized at a rate of 2.88 g h<sup>-1</sup>. O'Brien and co-workers have also successfully demonstrated the use of open-source software technologies in the synthesis of several benzamides, an improved automation system with an autosampling/product-collection system was described. The software was designed to select and load starting materials as well as collect products into separate collection flasks.<sup>163</sup>

Aka and co-workers have recently described a powerful automated flow-based strategy for identifying and optimizing

a cobalt-catalyzed oxidizing system for the bio-inspired dimerization of 2-propenyl phenols. They designed a reconfigurable flow reactor capable of online monitoring and process control. It was implemented as an automated screening platform to evaluate a matrix of 4 catalysts and 5 oxidants (plus the blank) at two different temperatures, resulting in an array of 50 reactions.<sup>164</sup>

## 7 In-line purification/downstream processing technologies in flow

Downstream processing and purification under flow conditions is typically characterised by chemical differentiation between reagents, products and by-products, and today the use of scavengers and catch-and-release approaches are commonplace in the field. The translation of more traditional purification techniques such as extraction, recrystallisation, distillation, filtration and chromatography which are largely based on the physical properties of molecules in large continue to prove challenging under flow conditions. The development of engineering solutions to overcome these shortcomings have seen growth in recent years as the drive to develop more integrated and truly continuous processes has increased.<sup>1</sup> Several pertinent examples of how these processes are being integrated into flow systems are discussed below including, solvent swapping approaches, liquid-liquid extraction devices, in-line crystallizations and triturations, in-line distillations, and in-line filtrations.

**7.1 Solvent swapping.** The ability to telescope different reactions together under flow conditions is reliant on either having solvent compatibility between the reactions or being able to swap solvents. In many instances solvent exchange is conveniently processed offline, however, if truly continuous uninterrupted processes are to be realised one needs to be

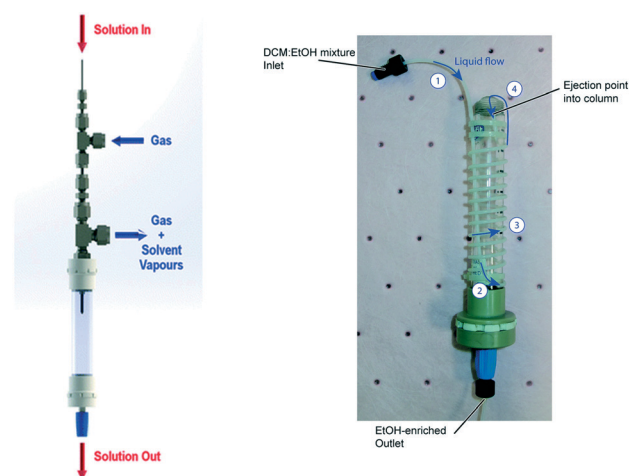


Fig. 6 Ley groups meso-fluidic aspirating evaporator (left) and single stage distillation column (right). Photographs reproduced with permission.<sup>160,164</sup>



able to efficiently effect continuous on-the-fly solvent swapping.

Ley and co-workers demonstrated an elegant solution through their use of a bespoke meso-fluidic evaporator wherein a reagent stream is aspirated to afford a high surface area spray inside a heated column module which is exposed to a desolvation gas that rapidly removes the solvent (Fig. 6).<sup>165</sup> The approach allows for rapid evaporation/concentration of the reagent stream and it can also be utilised to effect solvent swops through the introduction of a secondary solvent prior to entry into the evaporator. In this respect, the selective removal of the lower vapour pressure solvent can be achieved. The group utilised the approach during the synthesis of the neurotensin receptor-1, Meclintant (SR48692) in which they were able to successfully swap a toluene for methanol.<sup>166</sup>

The Ley group also developed a means of swapping solvents based on their boiling points using a single stage distillation column. In this instance PTFE tubing was wrapped around an Omnifit® column reactor and the end of the tubing was then directed into the top of the column module (Fig. 6).<sup>161</sup> The column was mounted into a heated (90 °C) jacket from a VapourTec R4+ unit. A solvent mix, dichloromethane and ethanol in the case reported were pumped into the coiled tubing. The lower boiling point solvent, dichloromethane rapidly boiled in the tubing ejecting the ethanol enriched reaction mixture into the centre of the column. The reaction mixture then exited the column out the bottom end, pumped directly into the next stage using a peristaltic pump.

In a similar vein Gruber-Woelfler and co-workers during the development of an approach for the continuous crystallisation of vitamin D<sub>3</sub> developed an evaporative solvent concentrator wherein a reagent stream is allowed to drop into a vertical heated column equipped with an internal thermocouple.<sup>167</sup> The column is fitted with a side-arm which is attached to a vacuum controller maintaining an internal pressure of 280 mbar. In this instance introduction of a mixed solvent system allows selective droplet evaporation of the solvent with the lower boiling point.

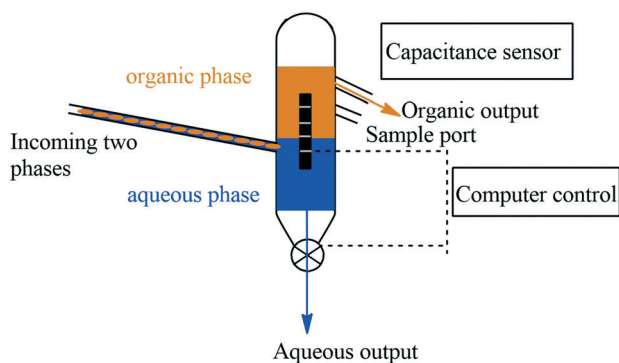


Fig. 7 An automated gravity-based separator by Adamo and co-workers.

**7.2 Liquid–liquid extractions.** Liquid–liquid extraction is one of the most fundamental and universally adopted separation techniques employed in synthetic chemistry and under batch conditions is readily implemented at both bench and industrial scales. Currently the two most common approaches to translation of liquid–liquid extractions to flow systems involve gravity-based separators which mimic separation funnels or membrane-based extractors.

In the first instance, as described earlier in this review Ley and co-workers have on several occasions demonstrated the use of in-line gravity-based extractors to effect liquid–liquid extractions, the operation of which has been automated using computer vision to track the solvent interface.<sup>159</sup> Adamo and co-workers fabricated an automated gravity-based separator that could be used in-line with continuous manufacturing, along with various filtration and crystallizing units. The gravity-based separator consisted of a Dean-Stark tube and a capacitive sensor that monitors the interface between the organic and aqueous streams (Fig. 7). The aqueous stream outlet was controlled to allow for complete separation between the aqueous stream and the organic streams.

The group also designed the well-known Zaiput liquid–liquid and gas–liquid in-line membrane-based separator. The separator was originally highlighted during the synthesis of fluoxetine hydrochloride and was designed to be chemically compatible by machining the wetted parts in perfluorinated polymers ethylene tetrafluoroethylene (ETFE) for the internal structure, PTFE for the porous membrane and PFA for the impermeable diaphragm of the pressure controller (Fig. 8).<sup>3</sup>

Syrris as part of their ASIA flow reactor series also developed a membrane-based separator called the FLEXX (flow liquid–liquid extraction) in which organic and aqueous phases are mixed and pumped across a membrane allowing diffusion to occur before splitting the stream into their constituent parts.<sup>168</sup> The membrane technology employed is notable in that it allows the separation of difficult to separate or miscible solvent systems such as THF and water (Fig. 9).

**7.3 Crystallization and trituration.** The ability to handle and process solids under flow conditions continues to prove challenging due to the microfluidic nature of the reactors in question, in recent times the development and use of reactors specifically designed to handle solids/precipitates have been reported, however, in practice their widespread adoption has to date not been realised.<sup>169,170</sup> The integration of semi-

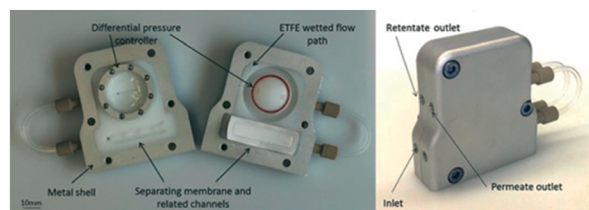
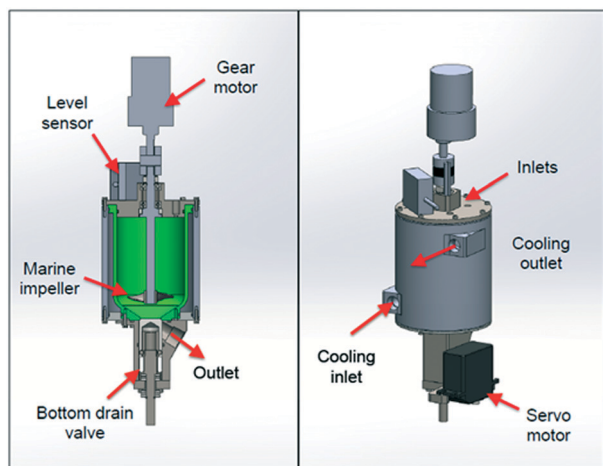
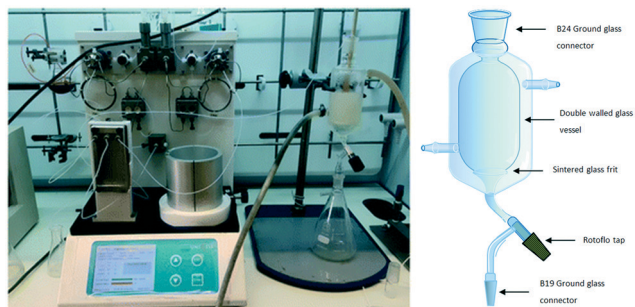


Fig. 8 Zaiput membrane separator by Adamo and co-workers. Photograph reproduced with permission.<sup>3</sup>



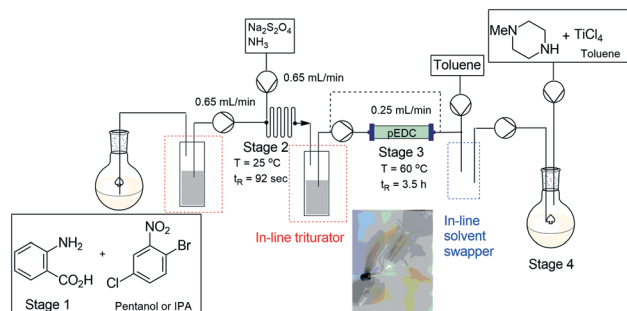


Fig. 9 Syrris Asia FLEXX.

Fig. 10 In-line crystallization under flow conditions by Adamo and co-workers. Image reproduced with permission.<sup>3</sup>Fig. 11 In-line double walled glass triturator. Photograph and image reproduced with permission.<sup>170</sup>

continuous and continuous crystallizers and tritulators has however seen more widespread development and adoption.

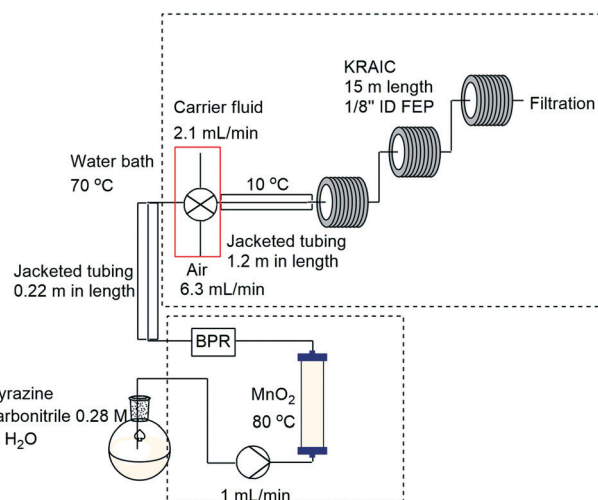
In most instances the use of miniaturized crystallization tanks allows the convenient crystallisation of material directly out of a flow reactor in a batch or semi-continuous manner.<sup>3</sup> Adamo and co-workers developed one such crystallisation device which was implemented in the downstream processing of lidocaine hydrochloride, diazepam, fluoxetine hydrochloride and diphenhydramine hydrochloride. The unit is comprised of a 120 mL jacketed HDPE (high density polyethylene) crystallizer was equipped with a PTFE coated marine impeller. The module is equipped with a level sensor and the temperature is controlled with a thermoelectric liquid cooler (LC-200, TE Technology, Inc.) to provide sufficient cooling capacity ensuring cooling rates below room temperature (Fig. 10).



Scheme 46 The synthesis of clozapine with purification/solvent swapping using an in-line triturator.

Utilising a similar approach our own research group demonstrated the synthesis of clozapine with in-line purification mediated in a semi-continuous fashion through the use of a trituration/solvent exchanger chamber.<sup>171</sup> The process allowed for the trituration of two intermediate products during the four-stage synthesis. The in-line triturator (Fig. 11) was constructed as a double walled glass vessel fitted with a sintered glass frit, the outlet of which was connected to a vacuum pump and the jacketed vessel could be attached to a separate cooling/heating unit. The process was affected through the introduction of the reagent stream to the cooled triturator which was pre-primed with an anti-solvent. Upon completion of the trituration process the filtrate was removed from the vessel under vacuum filtration. The chamber was then re-primed with a solubilising solvent allowing the dissolution of the trituated material prior to it being pumped into the next reaction stage (Scheme 46).

Scott and co-workers designed and demonstrated a system which allowed inline crystallisation in a truly continuous manner.<sup>172</sup> The approach involved the use of a tri-segmented tubular crystallizer (KRAIC) in the form of three coil reactors (1/8" ID FEP tubing, 15 m) in which the reaction mixture is segmented with air and an immiscible carrier solvent



Scheme 47 In-line crystallization of pyrazinamide.



allowing in-line crystallization. Notably the authors found it necessary to insert a section of jacketed tubing between the segmentor and the KRAIC which was cooled to 10 °C to ensure the rapid formation of large numbers of nuclei. This approach reduced crystallite size and was necessary to prevent blocking. The crystalliser was successfully used to purify pyrazinamide prepared upstream by reaction of pyrazinecarbonitrile with manganese (Scheme 47).

**7.4 Distillation.** The purification of chemical entities by distillation is readily achieved under batch-type processing conditions on both small and large scales, however, the application of in-line distillations in flow chemistry has remained largely limited. This may be due to the fact that one would typically need to couple in additional downstream processing operations such as solvent evaporation or phase separation prior to distillation of crude residues.

In terms of the application of distillations in flow several purification techniques have been developed to afford solvent swapping under micro-evaporation conditions several of which have been described previously in this article.<sup>161,165–167</sup> Hartman and co-workers used a novel approach when they designed a distillation device based upon a silicon microreactor with an integrated PTFE membrane (Fig. 12).<sup>173</sup> They demonstrated the distillation device by implementing a Heck transformation with aryl triflates. These transformations are commonly associated with chlorinated solvents. The formation of the triflate was performed in DCM, after which toluene (or DMF) was pumped into the reactor system. The reactor was heated to 70 °C allowing the DCM to vaporize and the aryl triflate along with the toluene to pass through the reactor. Gas-liquid segmented flow was established combining a nitrogen feeding line into the reactor. The device was designed such that the liquid flowed

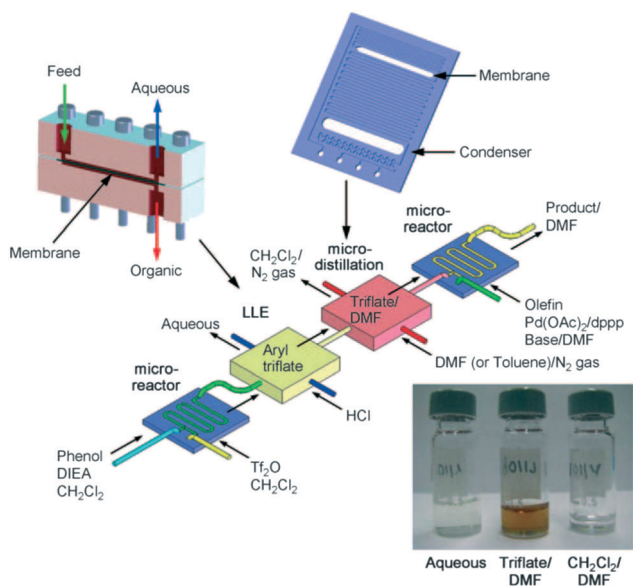
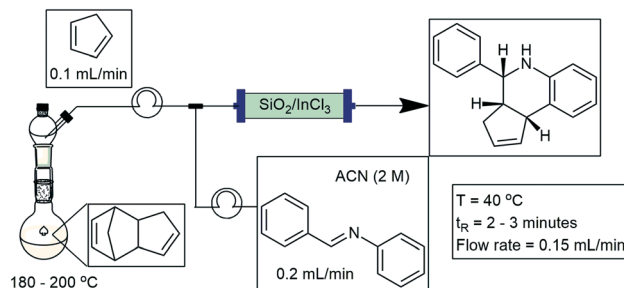


**Fig. 12** Distillation device based upon a silicon microreactor with an integrated PTFE membrane. Image and photograph reproduced with permission.<sup>172</sup>



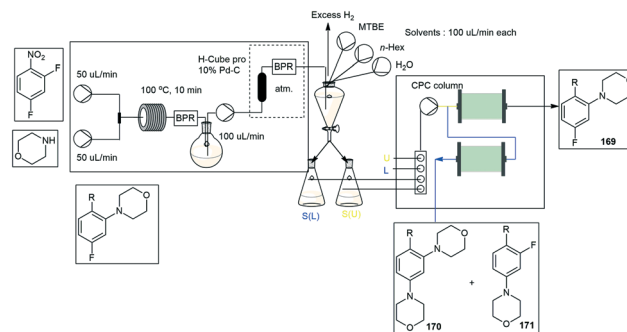
**Scheme 48** The use of an in-line distillate apparatus for the synthesis of quinoline derivatives.

through the integrated PTFE membrane and the vapour did not.

Although not an in-line distillation, Baumann and co-workers recently developed a platform that integrates reactive distillation with modern flow chemistry equipment.<sup>174</sup> In this instance, a Hickmann distillation apparatus was used to prepare pure cyclopentadiene by cracking. The distillate was collected at the rim of the top flask and was subsequently withdrawn *via* a side port in a continuous fashion. Several tetrahydroquinolines were generated through different aryl imines and cyclopentadiene were synthesized in this manner in yields of 75–90% (Scheme 48).

**7.5 Chromatography.** The purification of complex reaction mixtures in many instances requires more subtle separations that are not readily achievable using liquid-liquid extraction, filtration, distillation or crystallisation. In such case a chemist typically turns to chromatography which is readily implemented on bench-scale (albeit not so easily on scale) through simply batch-by-batch purification of crude reaction mixtures. The application of chromatographic purification protocols to flow systems is highly desirable, however, considering the continuous nature of flow chemistry, outside of catch-and-release chromatography it is not easily implemented.

Several reports have been described wherein a flow stream is directed into a series of simulated moving bed chromatography systems,<sup>175–178</sup> however, the complexity of such systems and the technical limitations leave one largely



**Scheme 49** In-line column chromatography demonstrated with a cross coupling reaction and hydrogenation [S(L) – lower layer, S(U) – upper layer].



restricted with regards to the separation of systems comprised of more than two components. An arguably more attractive approach is the use of centrifugal partition chromatography (CPC), such as was described by Greiner and co-workers wherein they were able to achieve a semi-continuous purification of aniline **169** which was produced in two steps under flow conditions (Scheme 49).<sup>179</sup> The final product stream was continuously collected and diluted with appropriate solvents to afford an appropriate biphasic liquid system prior to being pumped into a CPC column in a portion-wise fashion. Fortuitously, aniline **169** could readily be separated from by-products **170** and **171** in both ascending (eluted first) and descending (eluted last) mode. As such the purification protocol was readily automated, an initial sample injection was run in descending mode allowing the by-products to be washed out, thereafter a second sample injection occurred and the process was run in ascending mode allowing the isolation of the product **169** in 99.9% purity. The process was then repeatedly reverse cycled ultimately affording a 91% recovery of **169** after 5 h.

The Ley group in their efforts to purify more complex reaction matrices developed a semi-continuous supercritical fluid chromatography (SFC) system which notably allowed the isolation of material that did not elute either first or last and furthermore the group was able to successfully integrate the purification system between two discrete reactions (Scheme 50).<sup>180</sup> The system operated by allowing a crude reaction mixture to be continuously recirculated through the loading loops of four independent Rheodyne injection valves and each valve was in turn connected to a separate column housed in a heating oven. Switching a valve to its injection orientation allowed a SFC system to pump a sample of the crude mixture through the column whereafter a selection valve could be automated to allow the collection of up to five fractions.<sup>180</sup> The use of super critical carbon dioxide necessitated the need to separate the reaction mixture or purified fractions from gaseous carbon dioxide at points where system depressurization occurred, as such cyclone separators were inserted within the crude reaction mixture circulating loop directly after the Rheodyne injection valves, and after each of the final selection valves. The system was

automated in such a manner as to try stagger the injections between the Rheodyne valves to allow an almost constant output stream of material.

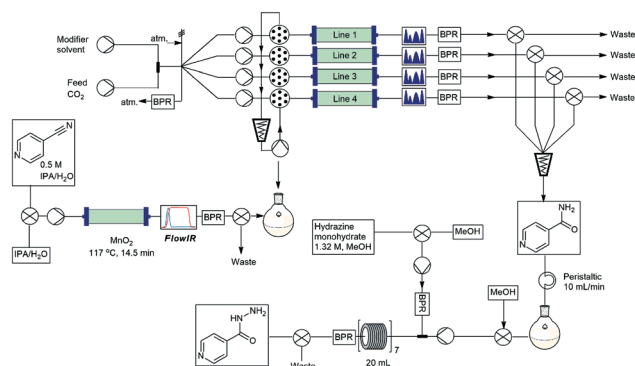
**7.6 Filtration.** Ley and co-workers used an integrated approach with several downstream modular components for the flow synthesis 2-aminoadamantane-2-carboxylic acid. One of the modular components that was used in the downstream processing, consisted of a motor and a PTFE scraper which was constructed as an inline filtration device.<sup>181</sup> A slurry stream was allowed to drip onto a sintered glass disk attached to a servo motor whose rotation was controlled using an Arduino circuit. As this disk rotated, solids accumulated on the surface of the sinter while liquids were able to pass through. A PTFE scraper mounted above the spinning disk was then used to remove the solid layer onto a replaceable filter paper. Liquid drops fell through holes cut into the filter paper and supporting PP mesh onto a cotton wool layer. A liquid reservoir collected filtrate from the base of the glass funnel structure.

## 8 Specialised flow reactors

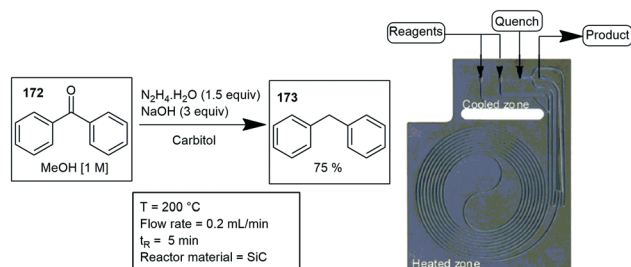
Lastly, we report on specialized flow reactors, designed for specific reaction applications or as a general reactor.

A few examples of microreactor etching are described below with Newman and Jensen demonstrating Wolff Kishner type reductions using a SiC etched microreactor. The reactor was designed to ensure general applicability to any reaction, which included two inlets, a quench line and an outlet. The cooled inlet and outlet zones were thermally separated from a spiral heated zone by a halo etch. The trapezoid-shaped channels amounted to an approximate 470  $\mu\text{L}$  internal volume. The microreactor demonstrated good corrosion resistance, typically problematic in glass and steel microreactors. Benzophenone **172** was reduced using hydrazine, carbitol and NaOH with a residence time of 5 min obtaining **173** in a 75% yield (Scheme 51).<sup>182,183</sup> Several more carbonyl compounds were reduced with yields ranging from 76–96%.<sup>184</sup>

Aminolysis of epoxides were performed at high temperatures and pressures with a silicon microreactor fabricated by deep reactive ion etching to form square cross section channels (400  $\mu\text{m}$  on the side), amounting to a reactor volume of 120  $\mu\text{L}$ . The inlet and outlet section of the reactor was compressed in an aluminum fluidic interface. They performed several epoxide

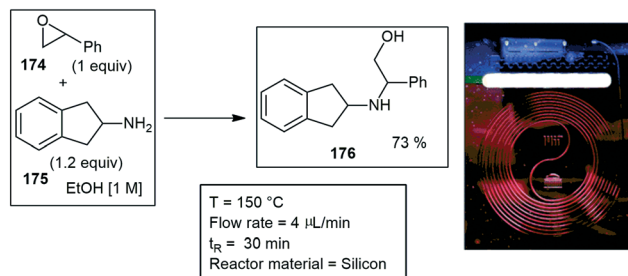


**Scheme 50** The use of super critical carbon dioxide for in-flow separations.

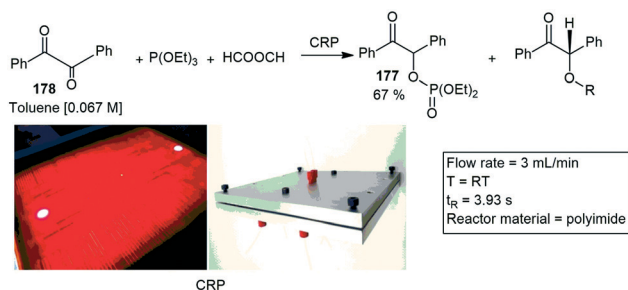


**Scheme 51** Silicon carbide microreactor custom built for general type applications.





**Scheme 52** Aminolysis of epoxides and amines. Photograph reproduced with permission.<sup>146</sup>



**Scheme 53** The use of super critical carbon dioxide for in-flow separations. Photograph reproduced with permission.<sup>187</sup>

aminolysis reactions, starting with the epoxide **174** and aniline **175** to form alcohol **176** (Scheme 52). During this reaction it was found that two other products could also be formed. Reactions were completed in under 5 min with excellent yields and conversions ranging from 66–84%.<sup>185,186</sup> The kinetics and scale-up of the epoxide aminolysis was investigated in a separate paper. The kinetic investigations showed that the activation energy for the formation of the desired product is observed to be higher than those for regio isomer formation and for secondary aminolysis, indicating that increasing temperature improves selectivity in addition to accelerating the reaction. A scale-up of this reaction was performed in a 12.5 mL steel tube mesoreactor, and 9 g of the product was produced in 30 min residence time.<sup>186</sup>

Reports of rapid flow chemistries aimed at performing reactions on millisecond time scales has also lend itself to specialised flow reactors designed to perform these ultra fast reactions. Kim and co-workers have reported a compact reaction module on a pad (CRP) with the following diameters, 170 × 170 × 1.2 mm. The CRP was utilized in the synthesis of  $\alpha$ -phosphonyloxy ketone **177**, an invaluable drug precursor. The basic architecture of the CRP is a channel for integrated micro-flow circuits between two banks of reactors, each bank containing a number of microreactors. The CRP system was devised by stacking 9 films of the patterned polyimide to integrate micro-flow circuits, combining the functions of the even distribution of feeds, being completely mixed in less than a few milliseconds. The drug precursor was synthesized in a few milli seconds equating to a production rate of 19.2 g h<sup>-1</sup> of the drug precursor **177**. The following reaction conditions were used: 0.067 M of **178** in

toluene with a flow rate of 3 mL min<sup>-1</sup> and a residence time of 3.93 s, which resulted in 67% yield of **177** (Scheme 53).<sup>187</sup>

Yoshida and co-workers being most prominent in the field of rapid microflow chemistries has recently synthesized afesal a bioactive molecule utilizing a polymer-based chip microreactor (CMR) with a 3D serpentine microchannel design. The internal volume of the CMR, 25 nL, is provided by the rectangular serpentine channels (width 200 μm, height 125 μm, length 1 mm). The Fries rearrangement was achieved on a sub millisecond time scale, providing a straightforward synthetic route for afesal. The rapid continuous flow nature of the CMR delivered a throughput of the product in 5.3 g h<sup>-1</sup>. Thus, we can assume by stacking multiple small and portable CMR systems, which individually fit in one hand, would have great potential for scalable industrial chemical synthesis.<sup>188</sup>

## Conclusion

Traditional organic synthesis methods are rapidly changing, and currently environmental concerns and impacts created by chemical manufacturers, and in particular by Big Pharma are being more heavily scrutinized than ever before. In today's world there is a drive for cleaner, safer, economical and conscientious chemical synthesis and manufacturing and this has in part been responsible for the rapid rise of flow chemistry and related technologies.

Although flow chemistry, in this the age of the fourth industrial revolution, is often seen as being the next evolutionary step in chemical manufacturing human resources are still just as important as material use, however, new these technologies and machines are transforming the way in which laboratory chemists work. Current evidence suggests a future in which the lines between chemistry and engineering are set to become more and more integrated from early on in process development and where the manufacture of chemical entities under continuous conditions is commonplace. That being said, despite some of the truly outstanding developments in the field much work still needs to take place in order to realise this. In particular, the development of truly continuous multi-step syntheses with integrated downstream processing and automation is today still challenging and by no means straightforward.

We hope that the works reported in this review paint a picture that serves as inspiration to synthetic chemists showing the vast scope of chemistries that now find themselves part of the flow chemistry family and highlight how the adoption of new technologies can benefit the modern chemist.

## Conflicts of interest

There are no conflicts to declare.

## Acknowledgements

This work was supported by the National Research Foundation of South Africa (grant number UID87893 and UID106959), the



University of Pretoria (University, Science Faculty Research Councils and Research and Development Program), South Africa and Pelchem Pty Ltd. Opinions expressed in this publication and the conclusions arrived at, are those of the authors, and are not necessarily attributed to the NRF.

## References

- S. V. Ley, D. E. Fitzpatrick, R. J. Ingham and R. M. Myers, Organic synthesis: march of the machines, *Angew. Chem., Int. Ed.*, 2015, **54**(11), 3449–3464.
- M. B. Plutschack, B. Pieber, K. Gilmore and P. H. Seeberger, The hitchhiker's guide to flow chemistry parallel, *Chem. Rev.*, 2017, **117**(18), 11796–11893.
- A. Adamo, R. L. Beingessner, M. Behnam, J. Chen, T. F. Jamison, K. F. Jensen, J. C. Monbaliu, A. S. Myerson, E. M. Revalor, D. R. Snead, T. Stelzer, N. Weeranoppanant, S. Y. Wong and P. Zhang, On-demand continuous-flow production of pharmaceuticals in a compact, reconfigurable system, *Science*, 2016, **352**(6281), 61–67.
- <https://www.worldofchemicals.com/media/iupac-names-top-10-emerging-technologies-in-chemistry/13101.html>, (accessed 20-12-2020).
- A. Macchi, P. Plouffe, G. S. Patience and D. M. Roberge, Experimental methods in chemical engineering: Microreactors, *Can. J. Chem. Eng.*, 2019, **97**(10), 2578–2587.
- C. O. Kappe, My twenty years in microwave chemistry: From kitchen ovens to microwaves that aren't microwaves, *Chem. Rec.*, 2019, **19**(1), 15–39.
- K. F. Jensen, Flow chemistry - Microreaction technology comes of age, *AIChE J.*, 2017, **63**(3), 858–869.
- T. Noel, Y. Cao and G. Laudadio, The fundamentals behind the use of flow reactors in electrochemistry, *Acc. Chem. Res.*, 2019, **52**(10), 2858–2869.
- C. Sambigioglio and T. Noël, Flow photochemistry: Shine some light on those tubes!, *Trends Chem.*, 2020, **2**(2), 92–106.
- Y. He, Y. Wu, J.-Z. Fu, Q. Gao and J.-J. Qiu, Developments of 3D printing microfluidics and applications in chemistry and biology: A review, *Electroanalysis*, 2016, **28**(8), 1658–1678.
- C. A. Hone and C. O. Kappe, The use of molecular oxygen for liquid phase aerobic oxidations in continuous flow, *Top. Curr. Chem.*, 2018, **377**(1), 2.
- M. Brzozowski, M. O'Brien, S. V. Ley and A. Polyzos, Flow chemistry: intelligent processing of gas-liquid transformations using a tube-in-tube reactor, *Acc. Chem. Res.*, 2015, **48**(2), 349–362.
- S. V. Ley, Y. Chen, D. E. Fitzpatrick and O. May, A new world for chemical synthesis?, *Chimia*, 2019, **73**(10), 792–802.
- C. Strauss, A continuous microwave reactor for laboratory-scale synthesis, *Chem. Aust.*, 1990, 186.
- T. Cablewski, A. F. Faux and C. R. Strauss, Development and application of a continuous microwave reactor for organic synthesis, *J. Org. Chem.*, 1994, **59**(12), 3408–3412.
- S.-T. Chen, S.-H. Chiou and K.-T. Wang, Preparative scale organic synthesis using a kitchen microwave oven, *J. Chem. Soc., Chem. Commun.*, 1990(11), 807–809.
- E. Thostenson and T.-W. Chou, Microwave processing: fundamentals and applications, *Composites, Part A*, 1999, **30**(9), 1055–1071.
- E. Comer and M. G. Organ, A microcapillary system for simultaneous, parallel microwave-assisted synthesis, *Chemistry*, 2005, **11**(24), 7223–7227.
- E. Comer and M. G. Organ, A microreactor for microwave-assisted capillary (continuous flow) organic synthesis, *J. Am. Chem. Soc.*, 2005, **127**(22), 8160–8167.
- G. Shore, S. Morin and M. G. Organ, Catalysis in capillaries by Pd thin films using microwave-assisted continuous-flow organic synthesis (MACOS), *Angew. Chem., Int. Ed.*, 2006, **45**(17), 2761–2766.
- W. S. Bremner and M. G. Organ, Multicomponent reactions to form heterocycles by microwave-assisted continuous flow organic synthesis, *J. Comb. Chem.*, 2007, **9**(1), 14–16.
- G. Shore, M. Tsimmerman and M. G. Organ, Gold film-catalysed benzannulation by microwave-assisted, continuous flow organic synthesis (MACOS), *Beilstein J. Org. Chem.*, 2009, **5**, 35.
- R. J. J. Jachuck, D. K. Selvaraj and R. S. Varma, Process intensification: oxidation of benzyl alcohol using a continuous isothermal reactor under microwave irradiation, *Green Chem.*, 2006, **8**(1), 29–33.
- M. C. Bagley, R. L. Jenkins, M. C. Lubinu, C. Mason and R. Wood, A simple continuous flow microwave reactor, *J. Org. Chem.*, 2005, **70**(17), 7003–7006.
- K. Engen, J. Sävmarker, U. Rosenström, J. Wannberg, T. Lundbäck, A. Jenmalm-Jensen and M. Larhed, Microwave heated flow synthesis of spiro-oxindole dihydroquinazolinone based IRAP inhibitors, *Org. Process Res. Dev.*, 2014, **18**(11), 1582–1588.
- V. Konda, J. Rydfjord, J. Sävmarker and M. Larhed, Safe palladium-catalyzed cross-couplings with microwave heating using continuous-flow silicon carbide reactors, *Org. Process Res. Dev.*, 2014, **18**(11), 1413–1418.
- M. Nishioka, M. Miyakawa, Y. Daino, H. Kataoka, H. Koda, K. Sato and T. M. Suzuki, Single-mode microwave reactor used for continuous flow reactions under elevated pressure, *Ind. Eng. Chem. Res.*, 2013, **52**(12), 4683–4687.
- G. Pipus, I. Plazl and T. Koloini, Esterification of benzoic acid in microwave tubular flow reactor, *Chem. Eng. J.*, 2000, **76**(3), 239–245.
- T. Ichikawa, M. Mizuno, S. Ueda, N. Ohneda, H. Odajima, Y. Sawama, Y. Monguchi and H. Sajiki, A practical method for heterogeneously-catalyzed Mizoroki–Heck reaction: Flow system with adjustment of microwave resonance as an energy source, *Tetrahedron*, 2018, **74**, 1810–1816.
- T. Ichikawa, T. Matsuo, T. Tachikawa, T. Yamada, T. Yoshimura, M. Yoshimura, Y. Takagi, Y. Sawama, J.-I. Sugiyama, Y. Monguchi and H. Sajiki, Microwave-mediated site-selective heating of spherical-carbon-bead-supported platinum for the continuous, efficient catalytic



- dehydrogenative aromatization of saturated cyclic hydrocarbons, *ACS Sustainable Chem. Eng.*, 2019, 7(3), 3052–3061.
- 31 I. R. Baxendale, C. M. Griffiths-Jones, S. V. Ley and G. K. Tranmer, Microwave-assisted Suzuki coupling reactions with an encapsulated palladium catalyst for batch and continuous-flow transformations, *Chemistry*, 2006, 12(16), 4407–4416.
- 32 P. He, S. J. Haswell and P. D. Fletcher, Microwave heating of heterogeneously catalysed Suzuki reactions in a micro reactor, *Lab Chip*, 2004, 4(1), 38–41.
- 33 P. He, S. J. Haswell and P. D. I. Fletcher, Microwave-assisted Suzuki reactions in a continuous flow capillary reactor, *Appl. Catal., A*, 2004, 274(1–2), 111–114.
- 34 F. Benaskar, N. G. Patil, V. Engels, E. V. Rebrov, J. Meuldijk, L. A. Hulshof, V. Hessel, A. E. H. Wheatley and J. C. Schouten, Microwave-assisted Cu-catalyzed Ullmann ether synthesis in a continuous-flow milli-plant, *Chem. Eng. J.*, 2012, 207–208, 426–439.
- 35 N. S. Wilson, C. R. Sarko and G. P. Roth, Development and applications of a practical continuous flow microwave cell, *Org. Process Res. Dev.*, 2004, 8(3), 535–538.
- 36 S. Yokozawa, N. Ohneda, K. Muramatsu, T. Okamoto, H. Odajima, T. Ikawa, J.-i. Sugiyama, M. Fujita, T. Sawairi, H. Egami, Y. Hamashima, M. Egi and S. Akai, Development of a highly efficient single-mode microwave applicator with a resonant cavity and its application to continuous flow syntheses, *RSC Adv.*, 2015, 5(14), 10204–10210.
- 37 M. Noshita, Y. Shimizu, H. Morimoto, S. Akai, Y. Hamashima, N. Ohneda, H. Odajima and T. Ohshima, Ammonium salt-accelerated hydrazinolysis of unactivated amides: Mechanistic investigation and application to a microwave flow process, *Org. Process Res. Dev.*, 2019, 23(4), 588–594.
- 38 P. Vámosi, K. Matsuo, T. Masuda, K. Sato, T. Narumi, K. Takeda and N. Mase, Rapid optimization of reaction conditions based on comprehensive reaction analysis using a continuous flow microwave reactor, *Chem. Rec.*, 2019, 19(1), 77–84.
- 39 B. Musio, F. Mariani, E. Śliwiński, M. A. Kabeshov, H. Odajima and S. V. Ley, Combination of enabling technologies to improve and describe the stereoselectivity of Wolff–Staudinger cascade reaction, *Synthesis*, 2016, 48(20), 3515–3526.
- 40 H. Egami, T. Sawairi, S. Tamaoki, N. Ohneda, T. Okamoto, H. Odajima and Y. Hamashima, (E)-3-[4-(Pent-4-en-1-yloxy)phenyl]acrylic Acid, *Molbank*, 2018, 2018(2), M996.
- 41 J. P. Barham, S. Tamaoki, H. Egami, N. Ohneda, T. Okamoto, H. Odajima and Y. Hamashima, C-Alkylation of N-alkylamides with styrenes in air and scale-up using a microwave flow reactor, *Org. Biomol. Chem.*, 2018, 16(41), 7568–7573.
- 42 H. Egami, S. Tamaoki, M. Abe, N. Ohneda, T. Yoshimura, T. Okamoto, H. Odajima, N. Mase, K. Takeda and Y. Hamashima, Scalable microwave-assisted Johnson–Claisen rearrangement with a continuous flow microwave system, *Org. Process Res. Dev.*, 2018, 22(8), 1029–1033.
- 43 J. P. Barham, S. Tanaka, E. Koyama, N. Ohneda, T. Okamoto, H. Odajima, J.-I. Sugiyama and Y. Norikane, Selective, scalable synthesis of C60-fullerene/indene monoadducts using a microwave flow applicator, *J. Org. Chem.*, 2018, 83(8), 4348–4354.
- 44 F. Bergamelli, M. Iannelli, J. A. Marafie and J. D. Moseley, A commercial continuous flow microwave reactor evaluated for scale-up, *Org. Process Res. Dev.*, 2010, 14(4), 926–930.
- 45 J. Moseley and E. Woodman, Scaling-out pharmaceutical reactions in an automated stop-flow microwave reactor, *Org. Process Res. Dev.*, 2008, 12, 967–981.
- 46 J. Moseley and E. Woodman, Energy efficiency of microwave- and conventionally heated reactors compared at meso scale for organic reactions, *Energy Fuels*, 2009, 23, 5438–5447.
- 47 R. Morschhäuser, M. Krull, C. Kayser, C. Boberski, R. Bierbaum, P. A. Püschner, T. N. Glasnov and C. O. Kappe, Microwave-assisted continuous flow synthesis on industrial scale, *Green Processes Synth.*, 2012, 1(3), 281–290.
- 48 K. Gilmore and P. H. Seeberger, Continuous flow photochemistry, *Chem. Rec.*, 2014, 14(3), 410–418.
- 49 A. Nakamura, K. Yoshida, S. Kuwahara and K. Katayama, Photocatalytic organic syntheses using a glass-milled microchip, *J. Photochem. Photobiol., A*, 2016, 322–323, 35–40.
- 50 Z. Meng, X. Zhang and J. Qin, A high efficiency microfluidic-based photocatalytic microreactor using electrospun nanofibrous TiO<sub>2</sub> as a photocatalyst, *Nanoscale*, 2013, 5(11), 4687–4690.
- 51 D. Rackl, P. Kreitmeier and O. Reiser, Synthesis of a polyisobutylene-tagged fac-Ir(ppy)<sub>3</sub> complex and its application as recyclable visible-light photocatalyst in a continuous flow process, *Green Chem.*, 2016, 18(1), 214–219.
- 52 R. S. Gonçalves, B. R. Rabello, G. B. César, P. C. S. Pereira, M. A. S. Ribeiro, E. C. Meurer, N. Hioka, C. V. Nakamura, M. L. Bruschi and W. Caetano, An efficient multigram synthesis of hypericin improved by a low power LED based photoreactor, *Org. Process Res. Dev.*, 2017, 21(12), 2025–2031.
- 53 F. R. Bou-Hamdan and P. H. Seeberger, Visible-light-mediated photochemistry: accelerating Ru(bpy)<sub>3</sub><sup>2+</sup>-catalyzed reactions in continuous flow, *Chem. Sci.*, 2012, 3(5), 1612–1616.
- 54 R. Telmesani, S. H. Park, T. Lynch-Colameta and A. B. Beeler, [2+2] Photocycloaddition of cinnamates in flow and development of a thiourea catalyst, *Angew. Chem., Int. Ed.*, 2015, 54(39), 11521–11525.
- 55 J. W. Tucker, Y. Zhang, T. F. Jamison and C. R. Stephenson, Visible-light photoredox catalysis in flow, *Angew. Chem., Int. Ed.*, 2012, 51(17), 4144–4147.
- 56 A. Kouridaki and K. Huvaere, Singlet oxygen oxidations in homogeneous continuous flow using a gas–liquid membrane reactor, *React. Chem. Eng.*, 2017, 2(4), 590–597.
- 57 B. Wriedt, D. Kowalczyk and D. Ziegenbalg, Experimental determination of photon fluxes in



- multilayer capillary photoreactors, *ChemPhotoChem*, 2018, 2(10), 913–921.
- 58 L. D. Elliott, M. Berry, B. Harji, D. Klauber, J. Leonard and K. I. Booker-Milburn, A small-footprint, high-capacity flow reactor for uv photochemical synthesis on the kilogram scale, *Org. Process Res. Dev.*, 2016, 20(10), 1806–1811.
- 59 L. D. Elliott, J. P. Knowles, P. J. Koovits, K. G. Maskill, M. J. Ralph, G. Lejeune, L. J. Edwards, R. I. Robinson, I. R. Clemens and B. Cox, Batch versus flow photochemistry: A revealing comparison of yield and productivity, *Chem. – Eur. J.*, 2014, 20(46), 15226–15232.
- 60 T. H. Rehm, C. Hofmann, D. Reinhard, H.-J. Kost, P. Löb, M. Besold, K. Welzel, J. Barten, A. Didenko and D. V. Sevenard, Continuous-flow synthesis of fluorine-containing fine chemicals with integrated benchtop NMR analysis, *React. Chem. Eng.*, 2017, 2(3), 315–323.
- 61 N. J. Straathof, Y. Su, V. Hessel and T. Noel, Accelerated gas-liquid visible light photoredox catalysis with continuous-flow photochemical microreactors, *Nat. Protoc.*, 2016, 11(1), 10–21.
- 62 N. J. Straathof, S. E. Cramer, V. Hessel and T. Noel, Practical photocatalytic trifluoromethylation and hydrotrifluoromethylation of styrenes in batch and flow, *Angew. Chem., Int. Ed.*, 2016, 55(50), 15549–15553.
- 63 G. Wu, T. Lv, W. Mo, X. Yang, Y. Gao and H. Chen, One-pot synthesis of tricyclo-1,4-benzoxazines via visible-light photoredox catalysis in continuous flow, *Tetrahedron Lett.*, 2017, 58(14), 1395–1398.
- 64 Y. Su, K. Kuijpers, V. Hessel and T. Noël, A convenient numbering-up strategy for the scale-up of gas-liquid photoredox catalysis in flow, *React. Chem. Eng.*, 2016, 1(1), 73–81.
- 65 J. S. Babra, A. T. Russell, C. D. Smith and Y. Zhang, Combining C-H functionalisation and flow photochemical heterocyclic metamorphosis (FP-HM) for the synthesis of benzo[1,3]oxazepines, *Tetrahedron*, 2018, 74(38), 5351–5357.
- 66 B. Shen, M. W. Bedore, A. Sniady and T. F. Jamison, Continuous flow photocatalysis enhanced using an aluminum mirror: Rapid and selective synthesis of 2'-deoxy and 2',3'-dideoxynucleosides, *Chem. Commun.*, 2012, 48(60), 7444–7446.
- 67 S. Jang, S. Vidyacharan, B. T. Ramanjaneyulu, K.-W. Gyak and D.-P. Kim, Photocatalysis in a multi-capillary assembly microreactor: toward up-scaling the synthesis of 2H-indazoles as drug scaffolds, *React. Chem. Eng.*, 2019, 4(8), 1466–1471.
- 68 K. C. Harper, E. G. Moschetta, S. V. Bordawekar and S. J. Wittenberger, A laser driven flow chemistry platform for scaling photochemical reactions with visible light, *ACS Cent. Sci.*, 2019, 5(1), 109–115.
- 69 C. J. Kong, D. Fisher, B. K. Desai, Y. Yang, S. Ahmad, K. Belecki and B. F. Gupton, High throughput photo-oxidations in a packed bed reactor system, *Bioorg. Med. Chem.*, 2017, 25(23), 6203–6208.
- 70 J. M. Tobin, T. J. D. McCabe, A. W. Prentice, S. Holzer, G. O. Lloyd, M. J. Paterson, V. Arrighi, P. A. G. Cormack and F. Vilela, Polymer-supported photosensitizers for oxidative organic transformations in flow and under visible light irradiation, *ACS Catal.*, 2017, 7(7), 4602–4612.
- 71 D. Cambie, F. Zhao, V. Hessel, M. G. Debije and T. Noel, A leaf-inspired luminescent solar concentrator for energy-efficient continuous-flow photochemistry, *Angew. Chem., Int. Ed.*, 2017, 56(4), 1050–1054.
- 72 D. Cambié, J. Dobbelaar, P. Riente Paiva, J. Vanderspikken, C. Shen, P. Seeberger, K. Gilmore, M. Debije and T. Noel, Energy-efficient solar photochemistry with luminescent solar concentrator based photomicroreactors, *Angew. Chem., Int. Ed.*, 2019, 58, 14374–14378.
- 73 C. A. Clark, D. S. Lee, S. J. Pickering, M. Poliakoff and M. W. George, A simple and versatile reactor for photochemistry, *Org. Process Res. Dev.*, 2016, 20(10), 1792–1798.
- 74 G. I. Ioannou, T. Montagnon, D. Kalaitzakis, S. A. Pergantis and G. Vassilikogiannakis, Synthesis of cyclopent-2-enones from furans using a nebulizer-based continuous flow photoreactor, *Org. Biomol. Chem.*, 2017, 15(48), 10151–10155.
- 75 A. Chaudhuri, K. P. L. Kuijpers, R. B. J. Hendrix, P. Shivaprasad, J. A. Hacking, E. A. C. Emanuelsson, T. Noël and J. van der Schaaf, Process intensification of a photochemical oxidation reaction using a Rotor-Stator Spinning Disk Reactor: A strategy for scale up, *Chem. Eng. J.*, 2020, 400, 125875.
- 76 M. Oelgemöller and D. Gurthie, *Continuous-flow photochemistry made easy with Vapourtec's photoreactor series*, 2020, vol. 97, pp. 38–42.
- 77 M. Baumann and I. R. Baxendale, Continuous photochemistry: the flow synthesis of ibuprofen via a photo-Favorskii rearrangement, *React. Chem. Eng.*, 2016, 1(2), 147–150.
- 78 J. W. Beatty, J. J. Douglas, K. P. Cole and C. R. Stephenson, A scalable and operationally simple radical trifluoromethylation, *Nat. Commun.*, 2015, 6, 7919.
- 79 I. Abdiaj and J. Alcazar, Improving the throughput of batch photochemical reactions using flow: Dual photoredox and nickel catalysis in flow for C(sp<sup>2</sup>)/C(sp<sup>3</sup>) cross-coupling, *Bioorg. Med. Chem.*, 2017, 25(23), 6190–6196.
- 80 H.-W. Hsieh, C. W. Coley, L. M. Baumgartner, K. F. Jensen and R. I. Robinson, Photoredox iridium–nickel dual-catalyzed decarboxylative arylation cross-coupling: From batch to continuous flow via self-optimizing segmented flow reactor, *Org. Process Res. Dev.*, 2018, 22(4), 542–550.
- 81 F. Lima, M. A. Kabeshov, D. N. Tran, C. Battilocchio, J. Sedelmeier, G. Sedelmeier, B. Schenkel and S. V. Ley, Visible light activation of boronic esters enables efficient photoredox C(sp<sup>2</sup>)-C(sp<sup>3</sup>) cross-couplings in flow, *Am. Ethnol.*, 2016, 128(45), 14291–14295.
- 82 I. Abdiaj, A. Fontana, M. V. Gomez, A. de la Hoz and J. Alcazar, Visible-light-induced nickel-catalyzed Negishi cross-couplings by exogenous-photosensitizer-free photocatalysis, *Angew. Chem., Int. Ed.*, 2018, 57(28), 8473–8477.



- 83 R. Xiao, J. M. Tobin, M. Zha, Y.-L. Hou, J. He, F. Vilela and Z. Xu, A nanoporous graphene analog for superfast heavy metal removal and continuous-flow visible-light photoredox catalysis, *J. Mater. Chem. A*, 2017, **5**(38), 20180–20187.
- 84 T. C. Sherwood, H. Y. Xiao, R. G. Bhaskar, E. M. Simmons, S. Zaretsky, M. P. Rauch, R. R. Knowles and T. G. M. Dhar, Decarboxylative intramolecular arene alkylation using N-(acyloxy)phthalimides, an organic photocatalyst, and visible light, *J. Org. Chem.*, 2019, **84**(13), 8360–8379.
- 85 C. Bottecchia, R. Martín, I. Abdiaj, E. Crovini, J. Alcazar, J. Orduna, M. J. Blesa, J. R. Carrillo, P. Prieto and T. Noël, De novo design of organic photocatalysts: Bithiophene derivatives for the visible-light induced C–H functionalization of heteroarenes, *Adv. Synth. Catal.*, 2019, **361**(5), 945–950.
- 86 Y. Chen, D. C. Blakemore, P. Pasau and S. V. Ley, Three-component assembly of multiply substituted homoallylic alcohols and amines using a flow chemistry photoreactor, *Org. Lett.*, 2018, **20**(20), 6569–6572.
- 87 Y. Chen, D. Cantillo and C. O. Kappe, Visible light-promoted beckmann rearrangements: Separating sequential photochemical and thermal phenomena in a continuous flow reactor, *Eur. J. Org. Chem.*, 2019, **2019**(11), 2163–2171.
- 88 I. Abdiaj, L. Huck, J. M. Mateo, A. de la Hoz, M. V. Gomez, A. Diaz-Ortiz and J. Alcazar, Photoinduced palladium-catalyzed Negishi cross-couplings enabled by the visible-light absorption of palladium-zinc complexes, *Angew. Chem., Int. Ed.*, 2018, **57**(40), 13231–13236.
- 89 X. J. Wei, I. Abdiaj, C. Sambiagio, C. Li, E. Zysman-Colman, J. Alcazar and T. Noel, Visible-light-promoted iron-catalyzed C(sp<sup>2</sup>)-C(sp<sup>3</sup>) Kumada cross-coupling in flow, *Angew. Chem., Int. Ed.*, 2019, **58**(37), 13030–13034.
- 90 Y. Chen, O. May, D. C. Blakemore and S. V. Ley, A photoredox coupling reaction of benzylboronic esters and carbonyl compounds in batch and flow, *Org. Lett.*, 2019, **21**(15), 6140–6144.
- 91 P. Vatankhah and A. Shamloo, Parametric study on mixing process in an in-plane spiral micromixer utilizing chaotic advection, *Anal. Chim. Acta*, 2018, **1022**, 96–105.
- 92 R. A. Green, R. C. D. Brown, D. Pletcher and B. Harji, A microflow electrolysis cell for laboratory synthesis on the multigram scale, *Org. Process Res. Dev.*, 2015, **19**(10), 1424–1427.
- 93 R. A. Green, K. E. Jolley, A. A. M. Al-Hadedi, D. Pletcher, D. C. Harrowven, O. De Frutos, C. Mateos, D. J. Klauber, J. A. Rincon and R. C. D. Brown, Electrochemical deprotection of para-methoxybenzyl ethers in a flow electrolysis cell, *Org. Lett.*, 2017, **19**(8), 2050–2053.
- 94 A. A. Folgueiras-Amador, K. Philipps, S. Guilbaud, J. Poelakker and T. Wirth, An easy-to-machine electrochemical flow microreactor: Efficient synthesis of isoindolinone and flow functionalization, *Angew. Chem., Int. Ed.*, 2017, **56**(48), 15446–15450.
- 95 C. Huang, X. Y. Qian and H. C. Xu, Continuous-flow electrosynthesis of benzofused S-heterocycles by dehydrogenative C-S cross-coupling, *Angew. Chem., Int. Ed.*, 2019, **58**(20), 6650–6653.
- 96 K. Arai, K. Watts and T. Wirth, Difluoro- and trifluoromethylation of electron-deficient alkenes in an electrochemical microreactor, *ChemistryOpen*, 2014, **3**(1), 23–28.
- 97 T. Arai, H. Tateno, K. Nakabayashi, T. Kashiwagi and M. Atobe, An anodic aromatic C,C cross-coupling reaction using parallel laminar flow mode in a flow microreactor, *Chem. Commun.*, 2015, **51**(23), 4891–4894.
- 98 J. Kuleshova, J. T. Hill-Cousins, P. R. Birkin, R. C. D. Brown, D. Pletcher and T. J. Underwood, The methoxylation of N-formylpyrrolidine in a microfluidic electrolysis cell for routine synthesis, *Electrochim. Acta*, 2012, **69**, 197–202.
- 99 R. A. Green, D. Pletcher, S. G. Leach and R. C. D. Brown, N-heterocyclic carbene-mediated oxidative electrosynthesis of esters in a microflow cell, *Org. Lett.*, 2015, **17**(13), 3290–3293.
- 100 R. A. Green, D. Pletcher, S. G. Leach and R. C. D. Brown, N-Heterocyclic carbene-mediated microfluidic oxidative electrosynthesis of amides from aldehydes, *Org. Lett.*, 2016, **18**(5), 1198–1201.
- 101 M. Ošeka, G. Laudadio, N. P. van Leest, M. Dyga, A. D. A. Bartolomeu, L. J. Gooßen, B. de Bruin, K. T. de Oliveira and T. Noël, Electrochemical Aziridination of Internal Alkenes with Primary Amines, *Chem*, 2021, **7**(1), 255–266.
- 102 J. Yu and J. Wu, Aziridination of Internal Alkenes Using Primary Alkyl Amines in a Microflow Electrocell, *Chem*, 2021, **7**(1), 18–19.
- 103 M. Kabeshov, B. Musio, P. Murray, D. Browne and S. Ley, Expedient preparation of nazlinine and a small library of indole alkaloids using flow electrochemistry as an enabling technology, *Org. Lett.*, 2014, **16**, 4618–4621.
- 104 M. Elsherbini, B. Winterson, H. Alharbi, A. A. Folgueiras-Amador, C. Genot and T. Wirth, Continuous-flow electrochemical generator of hypervalent iodine reagents: Synthetic applications, *Angew. Chem., Int. Ed.*, 2019, **58**(29), 9811–9815.
- 105 N. Amri, R. A. Skilton, D. Guthrie and T. Wirth, Efficient flow electrochemical alkoxylation of pyrrolidine-1-carbaldehyde, *Synlett*, 2019, **30**(10), 1183–1186.
- 106 C. T. Crowe, *Handbook, Multiphase Flow*, Taylor & Francis Group, New-York, 2006.
- 107 H. Seo, L. V. Nguyen and T. F. Jamison, Using carbon dioxide as a building block in continuous flow synthesis, *Adv. Synth. Catal.*, 2019, **361**(2), 247–264.
- 108 C. A. Hone and C. O. Kappe, Correction to: The use of molecular oxygen for liquid phase aerobic oxidations in continuous flow, *Top. Curr. Chem.*, 2019, **377**(2), 7.
- 109 B. Pieber, M. Shalom, M. Antonietti, P. H. Seeberger and K. Gilmore, Kontinuierliche heterogene photokatalyse in seriellen mikro-batch-reaktoren, *Angew. Chem.*, 2018, **130**(31), 10127–10131.
- 110 D. Cantillo, P. A. Inglesby, A. Boyd and C. O. Kappe, Hydrogen sulfide chemistry in continuous flow: Efficient



- synthesis of 2-oxopropanethioamide, *J. Flow Chem.*, 2017, **7**(2), 29–32.
- 111 M. Ramezani, M. A. Kashfipour and M. Abolhasani, Minireview: Flow chemistry studies of high-pressure gas-liquid reactions with carbon monoxide and hydrogen, *J. Flow Chem.*, 2020, **10**(1), 93–101.
- 112 C. Battilocchio, G. Iannucci, S. Wang, E. Godineau, A. Kolleth, A. De Mesmaeker and S. V. Ley, Flow synthesis of cyclobutanones via [2 + 2] cycloaddition of keteneiminium salts and ethylene gas, *React. Chem. Eng.*, 2017, **2**(3), 295–298.
- 113 Y. Wada, M. A. Schmidt and K. F. Jensen, Flow distribution and ozonolysis in gas-liquid multichannel microreactors, *Ind. Eng. Chem. Res.*, 2006, **45**(24), 8036–8042.
- 114 B. Gutmann, M. Köckinger, G. Glotz, T. Ciaglia, E. Slama, M. Zdravec, S. Pfanner, M. C. Maier, H. Gruber-Wölfler and C. Oliver Kappe, Design and 3D printing of a stainless steel reactor for continuous difluoromethylations using fluoroform, *React. Chem. Eng.*, 2017, **2**(6), 919–927.
- 115 J. Kobayashi, Y. Mori, K. Okamoto, R. Akiyama, M. Ueno, T. Kitamori and S. Kobayashi, A microfluidic device for conducting gas-liquid-solid hydrogenation reactions, *Science*, 2004, **304**(5675), 1305–1308.
- 116 P. Kluson, P. Stavarek, V. Penkavova, H. Vychodilova, S. Hejda and M. Bendova, Microfluidic chip reactor and the stereoselective hydrogenation of methylacetoacetate over (R)-Ru-BINAP in the [N 8222][Tf 2 N]/methanol/water mixed phase, *Chem. Eng. Process.: Process Intensif.*, 2017, **115**, 39–45.
- 117 J. Gardiner, X. Nguyen, C. Genet, M. D. Horne, C. H. Hornung and J. Tsanaktsidis, Catalytic static mixers for the continuous flow hydrogenation of a key intermediate of linezolid (zyvox), *Org. Process Res. Dev.*, 2018, **22**(10), 1448–1452.
- 118 C. Genet, X. Nguyen, B. Bayatsarmadi, M. D. Horne, J. Gardiner and C. H. Hornung, Reductive aminations using a 3D printed supported metal(0) catalyst system, *J. Flow Chem.*, 2018, **8**(2), 81–88.
- 119 C. H. Hornung, X. Nguyen, A. Carafa, J. Gardiner, A. Urban, D. Fraser, M. D. Horne, D. R. Gunasegaram and J. Tsanaktsidis, Use of catalytic static mixers for continuous flow gas-liquid and transfer hydrogenations in organic synthesis, *Org. Process Res. Dev.*, 2017, **21**(9), 1311–1319.
- 120 A. Avril, C. H. Hornung, A. Urban, D. Fraser, M. Horne, J. P. Veder, J. Tsanaktsidis, T. Rodopoulos, C. Henry and D. R. Gunasegaram, Continuous flow hydrogenations using novel catalytic static mixers inside a tubular reactor, *React. Chem. Eng.*, 2017, **2**(2), 180–188.
- 121 X. Nguyen, A. Carafa and C. H. Hornung, Hydrogenation of vinyl acetate using a continuous flow tubular reactor with catalytic static mixers, *Chem. Eng. Process.*, 2018, **124**, 215–221.
- 122 C. P. Park and D.-P. Kim, Dual-channel microreactor for gas-liquid syntheses, *J. Am. Chem. Soc.*, 2010, **132**(29), 10102–10106.
- 123 R. A. Maurya, C. P. Park and D.-P. Kim, Triple-channel microreactor for biphasic gas-liquid reactions: Photosensitized oxygenations, *Beilstein J. Org. Chem.*, 2011, **7**(1), 1158–1163.
- 124 H. Aran, D. Salamon, T. Rijnaarts, G. Mul, M. Wessling and R. Lammertink, Porous photocatalytic membrane microreactor (P2M2): a new reactor concept for photochemistry, *J. Photochem. Photobiol., A*, 2011, **225**(1), 36–41.
- 125 H. Aran, H. Klooster, J. Jani, M. Wessling, L. Lefferts and R. G. Lammertink, Influence of geometrical and operational parameters on the performance of porous catalytic membrane reactors, *Chem. Eng. J.*, 2012, **207**, 814–821.
- 126 P. Koos, U. Gross, A. Polyzos, M. O'Brien, I. Baxendale and S. V. Ley, Teflon AF-2400 mediated gas-liquid contact in continuous flow methoxycarbonylations and in-line FTIR measurement of CO concentration, *Org. Biomol. Chem.*, 2011, **9**(20), 6903–6908.
- 127 S. L. Bourne, P. Koos, M. O'Brien, B. Martin, B. Schenkel, I. R. Baxendale and S. V. Ley, The continuous-flow synthesis of styrenes using ethylene in a palladium-catalysed heck cross-coupling reaction, *Synlett*, 2011, **2011**(18), 2643–2647.
- 128 F. Mastronardi, B. Gutmann and C. O. Kappe, Continuous flow generation and reactions of anhydrous diazomethane using a teflon AF-2400 tube-in-tube reactor, *Org. Lett.*, 2013, **15**(21), 5590–5593.
- 129 M. O'Brien, N. Taylor, A. Polyzos, I. R. Baxendale and S. V. Ley, Hydrogenation in flow: Homogeneous and heterogeneous catalysis using Teflon AF-2400 to effect gas-liquid contact at elevated pressure, *Chem. Sci.*, 2011, **2**(7), 1250–1257.
- 130 M. O'Brien, I. R. Baxendale and S. V. Ley, Flow ozonolysis using a semipermeable teflon AF-2400 membrane to effect gas-liquid contact, *Org. Lett.*, 2010, **12**(7), 1596–1598.
- 131 B. Venezia, L. Panariello, D. Biri, J. Shin, S. Damilos, A. N. Radhakrishnan, C. Blackman and A. Gavriilidis, Catalytic Teflon AF-2400 membrane reactor with adsorbed ex situ synthesized Pd-based nanoparticles for nitrobenzene hydrogenation, *Catal. Today*, 2020, 104–112.
- 132 C. Xue, J. Li, J. P. Lee, P. Zhang and J. Wu, Continuous amination of aryl/heteroaryl halides using aqueous ammonia in a Teflon AF-2400 tube-in-tube micro-flow reactor, *React. Chem. Eng.*, 2019, **4**(2), 346–350.
- 133 H. Zhang, J. Yue, G. Chen and Q. Yuan, Flow pattern and break-up of liquid film in single-channel falling film microreactors, *Chem. Eng. J.*, 2010, **163**, 126–132.
- 134 N. Steinfeldt, R. Abdallah, U. Dingerdissen and K. Jähnisch, Ozonolysis of acetic acid 1-vinyl-hexyl ester in a falling film microreactor, *Org. Process Res. Dev.*, 2007, **11**, 1025–1031.
- 135 T. Rehm, S. Gros, P. Lob and A. Renken, Photonic contacting of gas-liquid phases in a falling film microreactor for continuous-flow photochemical catalysis with visible light, *React. Chem. Eng.*, 2016, **1**, 636–648.
- 136 A. Cantu-Perez, D. Ziegenbalg, P. Löb, A. Gavriilidis, V. Hessel and F. Schönfeld, Microstructure-based



- intensification of a falling film microreactor through optimal film setting with realistic profiles and in-channel induced mixing, *Chem. Eng. J.*, 2012, **179**, 318–329.
- 137 S. Ruwei, Q. Deng, R. Ding and L. Zhang, Generation of ethynyl grignard reagent in a falling film microreactor: An expeditious flow synthesis of propargyl alcohols and analogues, *Adv. Synth. Catal.*, 2014, **356**, 2931–2936.
- 138 D. Lokhat, A. Domah, K. Padayachee, A. Baboolal and D. Ramjugernath, Gas–liquid mass transfer in a falling film microreactor: Effect of reactor orientation on liquid-side mass transfer coefficient, *Chem. Eng. Sci.*, 2016, **155**, 38–44.
- 139 B. K. Vankayala, P. Löb, V. Hessel, G. Menges, C. Hofmann, D. Metzke, U. Krtischil and H.-J. Kost, Scale-up of process intensifying falling film microreactors to pilot production scale, *Int. J. Chem. React. Eng.*, 2007, **5**(1), 1–10.
- 140 M. De Sousa Duarte, M. Rolland, C. Sagnard, D. Suire, F. Flacher, O. Delpoux and C. P. Lienemann, High-pressure high-temperature transparent fixed-bed reactor for operando gas-liquid reaction follow-up, *Chem. Eng. Technol.*, 2019, **42**(3), 655–660.
- 141 D. A. Wenn, J. E. Shaw and B. Mackenzie, A mesh microcontactor for 2-phase reactions, *Lab Chip*, 2003, **3**(3), 180–186.
- 142 M. Irfan, T. N. Glasnov and C. O. Kappe, Continuous flow ozonolysis in a laboratory scale reactor, *Org. Lett.*, 2011, **13**(5), 984–987.
- 143 M. D. Roydhouse, A. Ghaini, A. Constantinou, A. Cantu-Perez, W. B. Motherwell and A. Gavriilidis, Ozonolysis in flow using capillary reactors, *Org. Process Res. Dev.*, 2011, **15**(5), 989–996.
- 144 V. Dragone, V. Sans, M. H. Rosnes, P. J. Kitson and L. Cronin, 3D-printed devices for continuous-flow organic chemistry, *Beilstein J. Org. Chem.*, 2013, **9**, 951–959.
- 145 C. R. Sagandira, M. Siyawanwaya and P. Watts, 3D printing and continuous flow chemistry technology to advance pharmaceutical manufacturing in developing countries, *Arabian J. Chem.*, 2020, **13**(11), 7886–7908.
- 146 S. Rossi, R. Porta, D. Brenna, A. Puglisi and M. Benaglia, Stereoselective catalytic synthesis of active pharmaceutical ingredients in homemade 3D-printed mesoreactors, *Angew. Chem., Int. Ed.*, 2017, **56**, 4290–4294.
- 147 J. S. Mathieson, M. H. Rosnes, V. Sans, P. J. Kitson and L. Cronin, Continuous parallel ESI-MS analysis of reactions carried out in a bespoke 3D printed device, *Beilstein J. Nanotechnol.*, 2013, **4**, 285–291.
- 148 M. R. Penny, Z. X. Rao, B. F. Peniche and S. T. Hilton, Modular 3D printed compressed air driven continuous-flow systems for chemical synthesis, *Eur. J. Org. Chem.*, 2019, **2019**(23), 3783–3787.
- 149 A. Zhakeyev, J. Tobin, H. Wang, F. Vilela and J. Xuan, Additive manufacturing of photoactive polymers for visible light harvesting, *Energy Procedia*, 2019, **158**, 5608–5614.
- 150 G.-N. Ahn, T. Yu, H.-J. Lee, K.-W. Gyak, J.-H. Kang, D. You and D.-P. Kim, A numbering-up metal microreactor for the high-throughput production of a commercial drug by copper catalysis, *Lab Chip*, 2019, **19**(20), 3535–3542.
- 151 H.-J. Lee, R. C. Roberts, D. J. Im, S.-J. Yim, H. Kim, J. T. Kim and D.-P. Kim, Enhanced Controllability of Fries Rearrangements Using High-Resolution 3D-Printed Metal Microreactor with Circular Channel, *Small*, 2019, **15**(50), 1905005.
- 152 Z. X. Rao, B. Patel, A. Monaco, Z. J. Cao, M. Barniol-Xicota, E. Pichon, M. Ladlow and S. T. Hilton, 3D-printed polypropylene continuous-flow column reactors: exploration of reactor utility in SNAr reactions and the synthesis of bicyclic and tetracyclic heterocycles, *Eur. J. Org. Chem.*, 2017, **2017**(44), 6499–6504.
- 153 H. Gong, B. P. Bickham, A. T. Woolley and G. P. Nordin, Custom 3D printer and resin for 18  $\mu\text{m}$  x 20  $\mu\text{m}$  microfluidic flow channels, *Lab Chip*, 2017, **17**(17), 2899–2909.
- 154 D. E. Fitzpatrick, M. O'Brien and S. V. Ley, A tutored discourse on microcontrollers, single board computers and their applications to monitor and control chemical reactions, *React. Chem. Eng.*, 2020, **5**(2), 201–220.
- 155 D. L. Browne, B. H. Harji and S. V. Ley, Continuous cold without cryogenic consumables: Development of a convenient laboratory tool for low-temperature flow processes, *Chem. Eng. Technol.*, 2013, **36**(6), 959–967.
- 156 M. O'Brien and D. Cooper, Continuous flow liquid-liquid separation using a computer-vision control system: The bromination of enamines with N-bromosuccinimide, *Synlett*, 2016, **27**(01), 164–168.
- 157 S. V. Ley, R. J. Ingham, M. O'Brien and D. L. Browne, Camera-enabled techniques for organic synthesis, *Beilstein J. Org. Chem.*, 2013, **9**, 1051–1072.
- 158 M. O'Brien, D. A. Cooper and J. Dolan, Continuous flow iodination using an automated computer-vision controlled liquid-liquid extraction system, *Tetrahedron Lett.*, 2017, **58**(9), 829–834.
- 159 R. J. Ingham, C. Battilocchio, J. M. Hawkins and S. V. Ley, Integration of enabling methods for the automated flow preparation of piperazine-2-carboxamide, *Beilstein J. Org. Chem.*, 2014, **10**, 641–652.
- 160 D. E. Fitzpatrick, C. Battilocchio and S. V. Ley, A novel internet-based reaction monitoring, control and autonomous self-optimization platform for chemical synthesis, *Org. Process Res. Dev.*, 2015, **20**(2), 386–394.
- 161 D. E. Fitzpatrick and S. V. Ley, Engineering chemistry: integrating batch and flow reactions on a single, automated reactor platform, *React. Chem. Eng.*, 2016, **1**(6), 629–635.
- 162 D. E. Fitzpatrick, T. Maujean, A. C. Evans and S. V. Ley, Across-the-world automated optimization and continuous-flow synthesis of pharmaceutical agents operating through a cloud-based server, *Angew. Chem., Int. Ed.*, 2018, **57**(46), 15128–15132.
- 163 M. O'Brien, A. Hall, J. Schrauwen and J. van der Made, An open-source approach to automation in organic synthesis: The flow chemical formation of benzamides using an inline liquid-liquid extraction system and a homemade 3-axis autosampling/product-collection device, *Tetrahedron*, 2018, **74**(25), 3152–3157.



- 164 E. C. Aka, E. Wimmer, E. Barre, N. Vasudevan, D. Cortes-Borda, T. Ekou, L. Ekou, M. Rodriguez-Zubiri and F. X. Felpin, Reconfigurable flow platform for automated reagent screening and autonomous optimization for bioinspired lignans synthesis, *J. Org. Chem.*, 2019, **84**(21), 14101–14112.
- 165 B. J. Deadman, C. Battilocchio, E. Sliwinski and S. V. Ley, A prototype device for evaporation in batch and flow chemical processes, *Green Chem.*, 2013, **15**(8), 2050–2055.
- 166 C. Battilocchio, B. J. Deadman, N. Nikbin, M. O. Kitching, I. R. Baxendale and S. V. Ley, A Machine-Assisted Flow Synthesis of SR48692: A Probe for the Investigation of Neurotensin Receptor-1, *Chem. – Eur. J.*, 2013, **19**(24), 7917–7930.
- 167 M. Escriba-Gelonch, V. Hessel, M. C. Maier, T. Noel, M. F. Neira d'Angelo and H. Gruber-Woelfler, Continuous-Flow In-Line Solvent-Swap Crystallization of Vitamin D3, *Org. Process Res. Dev.*, 2018, **22**(2), 178–189.
- 168 22-12-2020), h. w. s. c. p. a.-f.-c. a.
- 169 B. J. Deadman, D. L. Browne, I. R. Baxendale and S. V. Ley, Back Pressure Regulation of Slurry-Forming Reactions in Continuous Flow, *Chem. Eng. Technol.*, 2015, **38**(2), 259–264.
- 170 D. L. Browne, B. J. Deadman, R. Ashe, I. R. Baxendale and S. V. Ley, Continuous Flow Processing of Slurries: Evaluation of an Agitated Cell Reactor, *Org. Process Res. Dev.*, 2011, **15**(3), 693–697.
- 171 N. Neyt and D. Riley, Batch–flow hybrid synthesis of the antipsychotic clozapine, *React. Chem. Eng.*, 2018, **3**(1), 17–24.
- 172 C. D. Scott, R. Labes, M. Depardieu, C. Battilocchio, M. G. Davidson, S. V. Ley, C. C. Wilson and K. Robertson, Integrated plug flow synthesis and crystallisation of pyrazinamide, *React. Chem. Eng.*, 2018, **3**(5), 631–634.
- 173 R. L. Hartman, J. R. Naber, S. L. Buchwald and K. F. Jensen, Multistep microchemical synthesis enabled by microfluidic distillation, *Angew. Chem., Int. Ed.*, 2010, **49**(5), 899–903.
- 174 M. Baumann, Integrating reactive distillation with continuous flow processing, *React. Chem. Eng.*, 2019, **4**(2), 368–371.
- 175 A. G. O'Brien, Z. Horváth, F. Lévesque, J. W. Lee, A. Seidel-Morgenstern and P. H. Seeberger, Kontinuierliche synthese und aufreinigung durch direkte kopplung eines durchflussreaktors mit "simulated-moving-bed"-chromatographie, *Angew. Chem.*, 2012, **124**(28), 7134–7137.
- 176 J. W. Lee, Z. Horváth, A. G. O'Brien, P. H. Seeberger and A. Seidel-Morgenstern, Design and optimization of coupling a continuously operated reactor with simulated moving bed chromatography, *Chem. Eng. J.*, 2014, **251**, 355–370.
- 177 I. G. T. M. Penders, Z. Amara, R. Horvath, K. Rossen, M. Poliakoff and M. W. George, Photocatalytic hydroxylation of arylboronic acids using continuous flow reactors, *RSC Adv.*, 2015, **5**(9), 6501–6504.
- 178 B. Sreedhar, B. Shen, H. Li, R. Rousseau and Y. Kawajiri, Optimal design of integrated SMB-crystallization hybrid separation process using a binary solvent, *Org. Process Res. Dev.*, 2017, **21**(1), 31–43.
- 179 R. Örkényi, J. Éles, F. Faigl, P. Vincze, A. Prechl, Z. Szakács, J. Kóti and I. Greiner, Continuous synthesis and purification by coupling a multistep flow reaction with centrifugal partition chromatography, *Angew. Chem., Int. Ed.*, 2017, **56**(30), 8742–8745.
- 180 D. E. Fitzpatrick, R. J. Mutton and S. V. Ley, In-line separation of multicomponent reaction mixtures using a new semi-continuous supercritical fluid chromatography system, *React. Chem. Eng.*, 2018, **3**(5), 799–806.
- 181 R. J. Ingham, C. Battilocchio, D. E. Fitzpatrick, E. Sliwinski, J. M. Hawkins and S. V. Ley, A systems approach towards an intelligent and self-controlling platform for integrated continuous reaction sequences, *Angew. Chem.*, 2015, **127**(1), 146–150.
- 182 S. G. Newman, L. Gu, C. Lesniak, G. Victor, F. Meschke, L. Abahmane and K. F. Jensen, Rapid Wolff–Kishner reductions in a silicon carbide microreactor, *Green Chem.*, 2014, **16**(1), 176–180.
- 183 R. L. Hartman, J. R. Naber, N. Zaborenko, S. L. Buchwald and K. F. Jensen, Overcoming the challenges of solid bridging and constriction during Pd-Catalyzed C–N bond formation in microreactors, *Org. Process Res. Dev.*, 2010, **14**(6), 1347–1357.
- 184 D. Znidar, A. O'Kearney-McMullan, R. Munday, C. Wiles, P. Poehlauer, C. Schmoelzer, D. Dallinger and C. O. Kappe, Scalable Wolff–Kishner reductions in extreme process windows using a silicon carbide flow reactor, *Org. Process Res. Dev.*, 2019, **23**(11), 2445–2455.
- 185 M. W. Bedore, N. Zaborenko, K. F. Jensen and T. F. Jamison, Aminolysis of epoxides in a microreactor system: a continuous flow approach to  $\beta$ -amino alcohols, *Org. Process Res. Dev.*, 2010, **14**(2), 432–440.
- 186 N. Zaborenko, M. W. Bedore, T. F. Jamison and K. F. Jensen, Kinetic and scale-up investigations of epoxide aminolysis in microreactors at high temperatures and pressures, *Org. Process Res. Dev.*, 2011, **15**(1), 131–139.
- 187 S. J. Yim, B. T. Ramanjaneyulu, S. Vidyacharan, Y. D. Yang, I. S. Kang and D.-P. Kim, Compact reaction-module on a pad for scalable flow-production of organophosphates as drug scaffolds, *Lab Chip*, 2020, **20**(5), 973–978.
- 188 H. Kim, K.-I. Min, K. Inoue, D. J. Im, D.-P. Kim and J.-I. Yoshida, Submillisecond organic synthesis: Outpacing Fries rearrangement through microfluidic rapid mixing, *Science*, 2016, **352**(6286), 691.

